Vrije Universiteit Brussel

On the possible contribution of meteoritic metal to Ni-rich Indonesian kris daggers: Comparing original daggers and newly forged analog objects

Brandstätter, Franz; de Winter, Niels J.; Migliori, Alessandro; Padillia-Alvarez, Roman; Topa, Dan; Visser, Seerp; Goderis, Steven; Claeys, Philippe; Koeberl, Christian

Published in:
Meteoritics & planetary science

DOI:
10.1111/maps.14340

Publication date:
2025

License:
Unspecified

Document Version:
Accepted author manuscript

Link to publication

Citation for published version (APA):
Brandstätter, F., de Winter, N. J., Migliori, A., Padillia-Alvarez, R., Topa, D., Visser, S., Goderis, S., Claeys, P., & Koeberl, C. (2025). On the possible contribution of meteoritic metal to Ni-rich Indonesian kris daggers: Comparing original daggers and newly forged analog objects. *Meteoritics & planetary science*, *60*(5), 1023-1047. Article 14340. https://doi.org/10.1111/maps.14340

Copyright
No part of this publication may be reproduced or transmitted in any form, without the prior written permission of the author(s) or other rights holders to whom publication rights have been transferred, unless permitted by a license attached to the publication (a Creative Commons license or other), or unless exceptions to copyright law apply.

Take down policy
If you believe that this document infringes your copyright or other rights, please contact openaccess@vub.be, with details of the nature of the infringement. We will investigate the claim and if justified, we will take the appropriate steps.

Download date: 11. Nov. 2026

On the possible contribution of meteoritic metal to Ni-rich Indonesian kris daggers: Comparing original daggers and newly forged analog objects

Franz Brandstätter[1*], Niels J. de Winter[2,3], Alessandro Migliori[4], Roman Padillia-Alvarez[4], Dan Topa[1], Seerp Visser[5], Steven Goderis[3], Philippe Claeys[3] and Christian Koeberl[6]

[1]Natural History Museum Vienna, Burgring 7, 1010 Vienna, Austria

[2]Department of Earth Sciences, Vrije Universiteit Amsterdam, De Boelelaan 1086, 1081 HV Amsterdam, the Netherlands

[3]Archaeology, Environmental Changes and Geo-Chemistry group, Vrije Universiteit Brussel, Pleinlaan 2, 1050 Brussels, Belgium

[4]Department of Nuclear Sciences and Applications, International Atomic Energy Agency, Vienna International Centre, 1400 Vienna, Austria.

[5]Bellevuedreef 40, 2970 Schilde (Antwerp), Belgium

[6]Department of Lithospheric Research, University of Vienna, Althanstrasse 14, 1090 Vienna, Austria

Abstract

The "Weltmuseum Wien" owns a large collection of kris daggers from Indonesia. These objects are famous for their metal blades consisting of numerous layers made by a complicated forging process involving repeated folding and welding of the individual layers. There is a wide-spread belief that some krises were manufactured by adding meteoritic nickel-iron from the Prambanan meteorite that fell in Central Java and is known since the late 18th century. In our study, we investigated a selection of five Ni-rich krises from this collection with the aim to identify in their blades nickel-iron from Prambanan or another iron meteorite source. To obtain a better insight into the forging process, we investigated analog objects that were produced by a forging procedure similar to the one applied in the production of original krises, and by using iron meteorite material from the meteorites Campo del Cielo and Gibeon as admixture. These investigations were performed by non-destructive analytical techniques, including handheld X-ray fluorescence (HH-XRF) analysis, scanning electron microscopy (SEM), and electron microprobe (EMP) analysis. The original daggers were investigated by HH-XRF and micro-X-ray fluorescence (μ-XRF) analysis, as well as by portable laser ablation (pLA) sub-sampling followed by trace element analysis using inductively coupled plasma - mass spectrometry (ICP-MS). By comparing the data obtained for both materials we demonstrate that the main difficulties in identifying the presence of a meteoritic component in the kris daggers are due to the exclusive use of (quasi-)non-destructive methods in combination with locally varying surface heterogeneities, resulting from contamination, corrosion, and etching features. We also show that the presence of significant amounts of Ni and Co (in the wt% range) in a premodern kris dagger does not imply that it was manufactured with an admixture of meteoritic metal. We found that among the five krises investigated, only a single dagger (no. 900382) was manufactured with the possible admixture of nickel-iron from the Prambanan iron meteorite, as it contains high concentrations of siderophile elements and has a Ni/Co ratio comparable to that of the meteorite.

Introduction

The kris (or keris) is a distinct dagger indigenous to Southeast Asia (e.g., O'Connor, 1975). Being both a weapon and spiritual object, kris daggers are very strongly associated with the culture of Indonesia. In 2008, the importance of this cultural relationship was underlined by the inclusion of the Indonesian kris in the UNESCO representative list of the intangible cultural heritage of humanity (UNESCO Intangible Cultural Heritage, 2008, WWW document).

Typically, kris daggers have blades about 30 to 40 cm long that can be straight or wavy with a surface exhibiting a highly decorative pattern. This pattern is the result of a complicated forging process involving repeated folding and welding of individual layers consisting of two different metal types: iron or steel with a more etch-resistant metal alloy, the so-called *pamor* (see, e.g., Salvemini et al., 2020). The pattern itself is brought out on the blade's surface through the use of an etchant, often a mixture of arsenic and lime juice (Groneman, 1910), resulting in an intricate pattern of contrasting layers of etched-out, dark iron and the more etch-resistant lighter colored metal sort. Of special interest are kris daggers from the island of Java, as there is a wide-spread belief that several of them were made by using meteoritic nickel-iron as pamor material (e.g., Groneman, 1910; Bronson 1987). The only known local source from which meteoritic metal could have been taken is the Prambanan iron meteorite, which fell in the 18th century near the temple of Prambanan in central Java (Cohen 1905; Buchwald 1975). The exact date of the meteorite fall is unknown, but there are two slightly different estimates of it: Groneman (1910) mentions that it occurred during the reign of Sultan Pakubuwana II (1725 – 1749 CE), whereas according to Baumhauer (1866), the first news about the fall, described as a fireball event accompanied by the sound of thunder, reached the palace of Surakarta during the reign of Sultan Pakubuwana III (1749 – 1788 CE). The latter author further mentions that two iron masses were brought to Surakarta, a smaller one in 1784 CE and a larger one in 1797 CE. The first one soon disappeared, presumably being used by blacksmiths, while the second one was kept at the palace.

The "Weltmuseum Wien" (former Ethnological Museum) in Vienna, Austria, owns a large collection of Southeast Asian kris daggers. The aim of the present study was to identify daggers in this collection that contain nickel-iron metal from the Prambanan meteorite (which belongs to the "ungrouped" iron meteorite type, Kracher et al., 1980). However, due to a number of constraints, the identification of a meteoritic admixture in the kris blades is not a trivial task (e.g., Necmer et al., 2013). The main complications are the necessity for the exclusive use of non-destructive methods imposed by the value and uniqueness of the object, the size of the objects being ca. 30-40 cm in length, the identification of suitable areas/spots for chemical analysis, and the limitations inherent to the applied methods (e.g., spatial resolution and detection limits). In addition, a major difficulty in finding meteoritic pamor in a kris stems from the fact that a possible meteoritic admixture is present only as a minor component in the kris' blade. This contrasts with artefacts that were manufactured exclusively from iron meteorites – such as the Hopewell metal beads from Illinois (McCoy et al., 2017), various examples described by Buchwald (2005), or the famous Tutankhamun iron dagger (e.g., Comelli et al., 2016; Broschat et al., 2022). Confirming the presence of a meteoritic component in a kris can thus be considered a challenge, especially when unaltered metal is exposed only in some parts of the blade's surface. Thus, recent methods for the study of kris daggers comprise novel non-destructive methods (e.g., Salvemini et al., 2020) and the experimental study of analog materials (e.g., Ouzillou and Herd, 2024; Scheiblechner et al., 2022; Strobl et al., 2023).

In this work, we mainly used non-destructive X-ray fluorescence (XRF) analysis to investigate selected Indonesian kris daggers from the Weltmuseum Wien. This analytical technique has already been

proven useful for the classification of iron meteorites (e.g., Gemelli et al., 2014). Additionally, some early results of the kris dagger investigation were previously described in Brandstätter et al. (2016). In a first step, blades of about 200 Indonesian krises were semi-quantitatively checked for areas having significant Ni-contents (in the > 1 wt%-range) using handheld XRF spectroscopy (HH-XRF). After this preselection, five kris daggers and four artificial analog samples ("I", "II", "III" and "IV") that were made from terrestrial iron with admixtures of iron meteorite metal were selected for more detailed investigations. Four daggers and three analog samples (I, I, III) were investigated by HH-XRF, while all five daggers were studied by micro-XRF (μ-XRF) analysis. The analog samples I, II, and III, and the test sample (IV) that was manufactured as analog kris dagger, were also investigated by analytical scanning electron microscopy (ASEM) and by electron microprobe (EMP) analysis. Finally, trace element data from four krises were obtained using a portable laser ablation (pLA) unit combined with laboratory-based inductively coupled - plasma mass spectrometry (ICP-MS).

Samples and methods

Kris samples:

Photographs of the kris daggers investigated in this study are shown in Figure 1, and close-ups exhibiting details of some blades are presented in Figure 2. An overview of some basic information on the kris daggers selected from the collection of the Weltmuseum Wien is given in Table 1. All krises are from Java, except kris no. 900.382, which originates from the island of Sulawesi.
Kris no. 23606 (Figure 1a) is an asymmetric dagger having a 31 cm long straight to slightly curved blade and a black wooden hilt. The surface of the apparently intensely etched blade exhibits a marked pamor pattern consisting of an arrangement of subparallel lines that extend from the base to the tip (Figures 2a, 2f). According to the inventory entry from 1886, kris no. 23606 was manufactured in 1597 CE.

Kris no. 23646 (Figure 1b) is an asymmetric dagger having a 33.5 cm long straight to slightly curved blade and a black wooden hilt. The surface of the blade appears to be corroded and/or is in places covered with some kind of "patina" and exhibits a pamor pattern consisting of irregularly formed bright lines set in a dull brownish to greyish-black matrix (Figures 2b, 2g). The inventory entry from 1879 does not contain any information on when it was manufactured.

Kris no. 73397 (Figure 1c) is one of five kris daggers that were forged in 1904 by an *empu* (master blacksmith) in Yogyakarta, Java. The forging was commissioned by Franz Heger (director of the Ethnographic collection at the former k. k. Hofmuseum in Vienna) with the order to use meteoritic metal (from the local iron meteorite Prambanan) as pamor material (Groneman, 1910). The dagger has a 36 cm long straight to slightly curved blade and exhibits a pamor pattern that in places shows mirror symmetry (Figures 2c, 2h).

Kris no. 119014 (Figure 1d) is an asymmetric dagger having a 27.5 cm long straight to slightly curved blade and a light-brown wooden hilt. Its blade appears to be corroded exhibiting a dull greyish surface with brownish staining. The pamor pattern is not well developed and only a few shiny lines indicate the presence of blank metal (Figures 2d, 2i). The inventory entry from 1925 does not contain any information on when the dagger was manufactured.

Kris no. 900382 (Figure 1e) is an asymmetric dagger having a 29.5 cm long wavy blade and a brown wooden pistol-shaped hilt. The surface of the dagger exhibits a well-developed and highly decorative

pattern that apparently was achieved by intense etching of the blade (Figures 2e, 2j). The inventory entry from 1936 does not contain any information on when the dagger was manufactured.

Analog samples:

All analog samples were forged from malleable terrestrial iron with admixtures of metal from the iron meteorites Campo del Cielo and Gibeon. Material of both meteorites was obtained from private sources by S. Visser, who also performed the forging (Visser, 2021). References and compositional data for the different metal sources are given in Table 2. Three analog samples, consisting of puddle iron with admixtures of metal from the iron meteorites Campo del Cielo (sample I) and Gibeon (samples II, III), were obtained by a forging procedure (performed by S. Visser in 2015) similar to that applied in the production of "real" krises. In the case of sample I, about 15 g of Campo del Cielo material were enveloped by puddle iron and forged into a knife (Figure 3). For samples II and III, swarfs of Gibeon material (leftover from sawing) were filled into an envelope of puddle iron, which then was closed by electric welding. After repeated cycles of fire welding, forging out in length and folding, samples II and III consisted of puddle iron with 6 and 9 individual layers of Gibeon material, respectively.

Sample IV is from a test dagger (forged by S. Visser in 2018) that was manufactured by following the forging procedure as described in detail by Groneman (1910) for kris no. 73397. The starting materials for sample IV for making the analog dagger were low-carbon steel "ST37" and meteoritic metal consisting of about 90 vol% Campo del Cielo and 10 vol% Gibeon. At first, slices of Campo del Cielo were put into a flat steel box and filled up with swarfs of Gibeon material. After closing the box with a lid and after several cycles of fire welding, forging and drawing out, a 30 x 1.5 x 580 mm strip of pamor material consisting of steel and nine layers of meteoritic metal was obtained. The pamor material (subsample IV-0) was further on used to forge the test dagger by using steel "CK52" as non-meteoritic component. At consecutive stages of the forging procedure, several subsamples were taken. Generally, the later a subsample was taken during the manufacturing process, the more (and finer) pamor layers are present in it. Thus, the subsamples labelled IV-1, IV-2, IV-3 contain 2, 8, 16 pamor layers, respectively. In addition, subsamples were taken from the dagger's tang (the pointed end of the kris that is fitted into the handle) (IV-5) and from its tip (IV-6). All investigations (HH-XRF, ASEM, EMP) of the analog samples I, II, and III were performed on plain polished surfaces, whereas HH-XRF analysis was also performed on etched surfaces of these samples (labelled as Ic, IIc, IIIc).

Methods:

Four kris daggers (nos. 23606, 23646, 119014, 900382) and three test samples (I, II, III) were analyzed using HH-XRF. The measurements were performed using a Thermo Scientific Niton Xl3t XRF analyzer relying on a micro-X-ray tube with an Ag anode. The tube was operated at given sets of high voltage (maximum value 50 kV and not producing more than 2 W) in combination with metal filters to improve the excitation and detection of different groups of elements (measurement modes "High", "Main", "Low" and "Light"). All HH-XRF measurements were done using a spot size with a diameter of about 3 mm (the minimum allowed by the instrument). Several factory-made calibrations for the analysis of different types of samples are provided by the manufacturer. The calibrations are based on calculating the relative influence of a group of elements in each of the measurement channels. In the case of calibration for General Metals, which was used in this study, the mutual interferences between Fe, Ni, and Co seem to be well accounted for given the expected concentration intervals. It is worth to note that the probing depth varies depending on the energy of each element characteristic radiation used for the analysis (e.g., from about 4 µm for P-Kα to 45 µm for Ni-Kα) and

therefore the results of quantitative analysis might be influenced by a heterogeneous distribution in depth of the elements at sub-mm range. Instrumental detection limits (DL) for Fe, Ni, and Co were calculated based on the measurements of certified reference materials and by considering spectral interferences (e. g., Fe-Kβ with Co-Kα), and were determined to be 0.02 wt% for Fe, 0.002 wt% for Ni and 0.05 wt% for Co. In addition, as limit of quantification (QL) was considered a value corresponding three times the value of the respective DL and was calculated to be 0.06 wt% for Fe, 0.006 wt% for Ni and 0.15 wt%. These QLs are a useful threshold defining the concentration level above which the relative measurement uncertainty is better than 15 %. A detailed description of the certified reference materials and the calculations of the DLs is provided in the supplementary Appendix A. For a test sample from the Prambanan meteorite (NHM inventory no. D1483), the measured values for Ni (9.6 wt%) and Co (0.82 wt%) are in good agreement with the bulk data of Kracher et al. (1980) (Table 3).

Five kris daggers (nos. 23606, 23646, 73397, 119014, 900382) were analyzed using µ-XRF. The measurements were performed at the Vrije Universiteit Brussels using a M4 Tornado (Bruker Nano GmbH, Germany) benchtop device with a motorized X-Y-Z sample stage. The analyses (single points, line scans and area maps) were carried out with excitation based on a Rh anode operated at 50 kV, 600 µA (30 W) in combination with polycapillary X-ray optics, achieving a spot size of 25 µm. For quantitative point analysis, the measurement time (60 seconds) was optimized considering the trade-off between high sample throughput and low uncertainty following recommendations by de Winter et al. (2017). The quantification of the µ-XRF spectra was performed by using the Esprit software (Bruker Nano) that includes algorithms for peak deconvolution, integration of the net intensity of peaks, and determination of absolute elemental concentrations. A matrix-matched calibration for the elements Fe, Ni and Co was carried out using a set of six meteorite reference samples, namely IAB-main group Campo del Cielo (Wasson and Kallemeyn, 2002), ungrouped iron Gebel Kamil, IVA Gibeon (Gemelli et al., 2015), IVB Hoba (Campbell and Humayun, 2005), IIE Miles (Wasson, 2017) and IIAB North Chile (Wasson et al., 2007). Because of the overlap of the k-β peak of Fe with the k-α and k-β peaks used to quantify Co concentrations, the standard-based calibration for Co and (to a lesser extent) Ni was influenced by the concentrations of Fe in the standards. To circumvent this issue and to obtain more accurate results for Co and Ni, we constructed separate calibration lines for high-Fe (>90 wt% Fe) and lower Fe (<90 wt% Fe) standards in our dataset and used the appropriate calibration for our samples based on their observed Fe concentration. For the elements Fe, Ni and Co, the pooled standard deviation was calculated from the weighted averages of the variances of the analyzed meteorite standards. This pooled standard deviation was considered as a measure for the reproducibility of quantified Fe, Ni and Co concentrations in the analyzed materials, and resulted in a relative standard deviation of 0.34%, 3.21%, and 2.26% for Fe, Ni, and Co, respectively. The limits of detection for these three elements were determined to be 1.42 wt% for Fe, 1.43 wt% for Ni and 373 µg/g for Co based on this pooled standard deviation and on recommendations by Rousseau (2001), . All quantitative µ-XRF results and spreadsheets showing the calculations of the uncertainties and calibrations are provided in the supplementary Appendix A.

XRF maps were produced by scanning along the target area line-by-line, allowing the X-ray beam to dwell for only 1 ms per pixel to allow for larger areas to be scanned at 25 µm resolution. The concentration of elements in each individual pixel in the maps could not be quantified because the quality of the XRF spectrum collected at such short measurement time does not allow this. Instead, areas under the elemental peaks in the XRF spectrum were integrated and plotted as false-color images with color brightness proportional to the spectral intensity (see de Winter and Claeys, 2017).

The analog samples were investigated at the Natural History Museum, Vienna, by using a Jeol JXA-8530F field emission electron microprobe and a Jeol JSM-6610LV analytical electron microscope. Electron microprobe analyses were carried out by using Jeol and Probe for EMP software at operation conditions of 15 kV (samples I, II, III) and 25 kV (sample IV) accelerating voltage, a beam current of 20

nA and a spot size of 1 µm. For all analog samples, concentrations of Fe, Ni and Co were measured. In the case of samples I, II, III, the concentrations of Si, Cr, and Mn were also determined to recognize possible "mixed" analyses of iron metal and slag inclusions within the puddle iron. Emission lines and standards used were Si-Kα and Fe-Kα (Si-bearing iron metal), Cr-Kα (chromite), Mn-Kα (tephroite), Ni-Kα (nickel metal), and Co-Kα (cobalt metal). Detection limits for the measurements at 15 kV were determined to be 0.004 wt% Si, 0.02 wt% Fe, 0.016 wt% Ni, 0.016 wt% Co, 0.015 wt% Mn and 0.01 wt% Cr. For measurements at 25 kV, detection limits were determined to be 0.04 wt% Fe, 0.03 wt% Ni, and 0.03 wt% Co. Estimated sampling depths for measurements at 15 kV and 25 kV are about 1 µm and 2 µm, respectively.

Four krises (nos. 23606, 23646, 119014, 900382) and one polished slab of the Prambanan meteorite (NHMV inventory no. D1483) were analyzed by pLA-ICP-MS (Glaus et al. 2012). In a first step, the objects were sampled at the Natural History Museum, Vienna by a portable laser ablation device as described in detail by Numrich et al. (2024). The pLA setup consisted of a diode pumped solid state laser producing pulsed green light. The laser was coupled via a lens mounted on an xy-stage with an optical glass fiber to focus the laser light onto the sample surface. To find suitable sampling spots, a monochromatic CCD camera mounted on top of the ablation head was used, allowing the observation of ca. 1 mm^2 magnified surface area, that was illuminated by an LED ring mounted inside the ablation head. The laser bombardment resulted in cone-shaped ablation craters with a diameter of 100 µm and a depth of about 150 µm. The ablated material was collected by suction through a silicon tube and deposited on hydrophilic polycarbonate membrane filters, whereas from each object, the ablated material of four spots was collected as one bulk sample on a filter wheel. After sampling, the bulk samples were stored in sealed containers for further treatment and ICP-MS analysis at the Curt-Engelhorn-Center in Mannheim, Germany. There, the filter with the deposited ablation aerosol was transferred to a 2 ml Safelock tube (Eppendorf) and treated overnight with 1:1 diluted aqua regia. The following day, the filter was removed from the Safelock tube, the aqua regia was evaporated, and the residue was directly taken up in 6N HCl. Just before the measurements, the solution was diluted to 0.5N HCl. This treatment was also applied to various gold standards to control the quality of the chemical preparation. Concentrations of Fe, Ni, Co, and selected trace elements (Table 5) were determined using a Thermo Fisher Scientific ICAPQ quadrupole inductively coupled plasma-mass spectrometer with collision cell technology (CCT), whereas all analyzed element abundances were normalized to 100 % to obtain concentrations in the solid sample. Plasma power was 1400 W and flow rates of the plasma gas, auxiliary gas, and nebulizer gas were 13 L/min, 0.7 L/min, and 0.9 L/min, respectively.

Results and discussion

General considerations

We first discuss some general considerations that have relevance for the interpretation of the possible origin of the investigated kris daggers, namely

i. The age of manufacturing of the selected objects
ii. The presence of non-meteoritic Ni (and Co) in pre-modern krises
iii. Quantification of a possible meteoritic component in a kris blade

i) It is well known that Indonesian kris daggers can be traced back to at least the 14th century (e.g., O'Connor, 1975; Necemer et al., 2013; Salvemini et al., 2020). However, not all of the inventory entries of museum collections contain data on the exact origin and/or age of the inventoried daggers. For instance, for the five daggers from the Weltmuseum Wien investigated in this study (Table 1), the inventory book contains the year of acquisition of these objects, but an age is given for only two of

the daggers. The only documented local Indonesian source for meteoritic pamor material is the Prambanan iron meteorite, which fell in the mid-18th century (see above). Thus, the late 18th century forms an earlier time limit before which no Indonesian kris may contain iron from any known meteorite (Bronson, 1987).

ii) In terms of major element chemistry, Ni and Co are (besides Fe) the most abundant metals in iron meteorites (e. g., Wasson, 1985) and thus the main elements that have to be considered for a possible meteoritic admixture in kris daggers. However, it cannot generally be excluded that Ni (and Co) of terrestrial origin were added during the making of kris blades. Nickel-containing iron did not reach Indonesia before the 1890s when in Europe Ni-steel was produced on a commercial scale (Bronson, 1987). Thus, for a premodern (here defined as manufactured before 1890) kris dagger, Ni-bearing pamor material can only originate from either meteoritic or locally smelted iron. For the latter, the only sources in question are ores from lateritic deposits. Indonesia is known for several occurrences of Ni laterite ore deposits (e.g., Butt and Cluzel, 2013; van der Ent et al., 2013; Zhang et al., 2020). Modern industrial Ni mining has a long history in Indonesia, which started in the early 1900s, whereas at present most lateritic Ni mining takes place at Soroaka on the island of Sulawesi (van der Ent et al., 2013). Interestingly, there is evidence that by 1800 central Sulawesi had long been an important regional center of iron production and references to iron exports from Sulawesi go back even as far as the early 1500s (Bronson, 1987). Since the end of the 19th century, material from the Prambanan meteorite obtained the status as the "true" pamor for precious kris daggers. However, although the meteorite had fallen in the second half of the 18th century, before the mid-19th century, the only "true" pamor known to Europeans and most South Asians was iron metal mostly from Sulawesi (Bronson, 1987). Contents of Ni and Co in lateritic ores are relatively low when compared to meteoritic iron. For 20 globally distributed lateritic deposits (Elias, 2002), typical concentrations ranges expressed in ore grades are 1-2.6 wt% Ni and 0.05-0.18 wt% Co, with corresponding Ni/Co ratios in the range of 9-17. For different size fractions of the lateritic ore, a detailed mineralogical study of the Indonesian Weda Bay nickel laterite deposit yielded concentrations in the range of 7.8-31.7 wt% Fe, 2.1-3.3 wt% Ni, and 0.1-0.5 wt% Co, while the bulk of the ore contains 28.9 wt% Fe, 2.5 wt% Ni, and 0.2 wt% Co with a typical Ni/Co ratio of 12.5 (Farrokhpay et al., 2019). This is close to the Ni/Co ratio of 14.4 measured for Prambanan (Kracher et al., 1980).

iii) For the quantitative determination of a possible meteoritic admixture in kris daggers, various aspects/facts should be considered. Iron meteorites consist almost entirely of siderophile elements and typically contain bulk concentrations of about 90 wt% Fe, 5-10 wt% Ni, 0.4-0.6 wt% Co, and trace amounts of other siderophile and chalcophile elements (e.g., Wasson, 1985; Wasson et al., 1998 and references therein). Certain trace elements, such as Ga and Ge (together with Ni), are used to classify iron meteorites in chemical groups, whereas their bulk concentrations vary by more than five orders of magnitude within the iron meteorite population but show narrow concentration ranges within almost all groups, while other elements, such as Ir, can show a wide range within a single iron meteorite group (e. g., Wasson, 1985). In addition, the structural classification of an iron meteorite (Buchwald, 1975) should be considered, as the structural type is an approximate measure for the "coarseness" of the meteorite's texture and thus for its homogeneity on a cm to sub-mm scale. Prambanan, the only meteorite considered for Indonesian krises, is classified as an ungrouped iron with bulk concentrations of 10.1 wt% Ni and 0.7 wt% Co (Kracher et al., 1980) and as a finest octahedrite with a bandwidth of 125 ± 50 µm (Buchwald, 1975). It thus can be assumed that quantitative spot analyses in the 100 µm to mm size on small Prambanan samples should yield element concentrations which are close to those of its bulk composition values. According to

Buchwald (1975), it appears that all Prambanan specimens present in collections have been artificially heated and partially forged, whereas schreibersite, previously existing as 0.1-0.2 mm blebs in intersections of kamacite lamella, was mainly destroyed and dissolved. Thus, it seems rather unlikely that previously occurring phosphides and/or sulfides (e.g., troilite) survived the forging process of kris daggers that involves cycles of repeated welding. However, when Prambanan metal is present as pamor in a kris dagger, varying proportions of the meteoritic component and the host iron metal can be expected to occur in the sub-mm range, affecting the ratios of metals analyzed in each spot analysis. Therefore, some criteria, such as the use of Ni/Fe and Ni/Co ratios to distinguish between iron meteorites and Ni-bearing iron artefacts (e.g., Jambon, 2017) are not applicable in all cases or should be carefully evaluated. One should also consider that the surface of the investigated blades can have an uneven topography (being problematic for non-destructive surface techniques), which is often the result of extensive etching. Etching itself can also lead to selective dissolution of certain elements, and thus to a change in the observed elemental concentrations and ratios.
Further aspects that should be considered are the different spot diameters and sampling depths of the applied methods in this study. EMP analysis was performed with a spot size of about 1 µm and sampling depths in the range 1 -2 µm, allowing the investigation of compositional changes on the µm-scale without significant influence from any heterogeneity in depth. By far the largest spot size (3 mm) was used for HH-XRF analysis with a sampling depth of about 50 µm for Ni and Co. The µ-XRF measurements were performed at a much smaller spot size of 25 µm but with approximately the same sampling depth. Therefore, µ-XRF spots should be small enough to excite zones of the kris blade that are exclusively composed of pamor material, but the quantitative results are likely influenced by compositional heterogeneity in depth. Sampling by laser ablation produced a 100 µm large spot reaching a sampling depth of about 150 µm. For each kris dagger, material from four spots was combined for pLA-ICP-MS as a single bulk analysis. As a result, the information about the chemical composition of the individual spots was lost. However, this disadvantage is largely compensated by significantly lower detection limits of minor and trace element concentrations determined by pLA-ICP-Ms (Table 5) when compared to the concentrations obtained by XRF-methods in the present study.

Analog samples I, and II, III

The detailed ASEM and EMP investigation of the Ni-rich layers in analog samples I, and II, III revealed that meteoritic nickel-iron was redistributed within the layers (Figure 4) during the repeated process of fire welding and forging. Typically, the thin layers (average thickness <1 mm) are chemically zoned (Figure 5) with highly variable Ni concentrations. Measured maximum contents of Ni are 40 wt%, 8 wt%, 23.8 wt% in samples I, II, III, respectively. High concentrations of Ni are mainly restricted to a narrow rim within the meteoritic layer at the contact zone to the adjacent puddle iron (e. g., Figure 5; spots 3,4, 14, 15). While it is evident that the forging of the analog materials led to a redistribution of Ni and Co in the layers containing meteoritic admixtures (Campo del Cielo in sample I and Gibeon in samples II and III), there apparently occurred no significant diffusion of these elements into the adjacent puddle iron (e. g., Figure 5; spots 16, 17). This observation has a direct implication for the interpretation of XRF measurements of kris daggers. Provided that the iron dominated host metal of the pamor layers in a kris blade does not contain significant amounts of Ni and Co and, taking into account that the diameter of an analysis spot significantly exceeds the average thickness of the exposed pamor lines (especially in the case of HH-XRF), the measured concentrations of these elements can be expected to mainly depend on the ratio of host metal to pamor material in the analyzed spot. Therefore, the Ni/Co ratio should be approximately constant in such analyses.

In accordance with this assumption, the investigation of analog materials by HH-XRF and EMP analyses (Table 4a, Figure 6) has shown that the concentrations of Ni and Co in the analyzed spots are – as expected - positively correlated and closely resemble the bulk Ni/Co ratio of the respective meteoritic admixture. The diameter of the analysis spots for HH-XRF measurements and EMP analysis was 3 mm and 1 µm, respectively. Thus, in a Co vs. Ni diagram (Figure 6) almost all of the HH-XRF analyses, except those of the etched samples (Ic, IIc, IIIc), plot below the bulk concentrations of these elements in the respective meteorite admixture. The significantly higher Ni/Co ratios of the etched analog samples are likely a consequence of selective etching that locally enriches the more etch-resistant Ni. Electron microprobe analyses exhibit the same Ni/Co ratios as the HH-XRF data in the low Ni-range (Ni < 10 wt%) but deviate to higher Ni/Co ratios with increasing Ni-content (Figure 6). The latter behavior of the Ni/Co ratios can be explained by the preferred enrichment of Co in kamacite compared to taenite (Rasmussen et al. 1988).

Analog dagger IV

In contrast to test samples I, II, and III, sample IV was manufactured in a more complicated forging procedure. In a first step, the meteoritic admixture consisting of about 90 vol% of Campo del Cielo and 10 vol% Gibeon, was forged together with steel ST37 to obtain a multi-layered composite (subsample IV-0) that then was used as pamor material for forging the blade of the analog dagger from steel CK52. The texture of the subsamples (Figure 7) that were taken at consecutive stages during the forging process exhibits the increasing thinning of the individual pamor lines within these composite materials. For example, in samples IV-1, IV-2, and IV-3 the approximate thickness of the pamor lines is 800 µm, 100 µm, and 50 µm, respectively. The thinning of the pamor lines is accompanied by a corresponding decrease of the respective spacing between them (Figures 7 c, d). In terms of chemical composition (determined by EMP analysis), the subsamples of dagger IV and the analog samples I, II, and III are very similar. The former also has positively correlated concentrations of Ni and Co (Figure 8) that plot closely along the bulk Ni/Co ratio line in the low Ni-range (Ni < 10 wt%) of the respective meteoritic admixture and deviate to higher Ni/Co ratios at higher Ni-contents with up to 23 wt% Ni. Three distinct compositional clusters can be distinguished in the Co versus Ni plot: (i) analyses of spots in the steel matrix and/or close to the boundary between steel matrix and pamor line plot at very low Ni concentrations; (ii) analyses performed on the tang (sample IV-5) and on the tip (sample IV-6, Figure 9) – both samples were taken during the late stage of forging – plot in the 3.5-5 wt% Ni concentration range; (iii) as Campo del Cielo is the dominant component in the pamor material of dagger IV, the third cluster correspondingly plots close to its bulk composition. All analyses that plot at Ni > 10 wt% are from samples that were taken during early stages of forging.

XRF-analyses and pLA-ICP-MS analyses of kris blades

In this section, the results of the HH-XRF and µ-XRF measurements, as well as pLA-ICP-MS data, are discussed for each individual kris dagger, with a focus on the respective elemental concentrations of Ni, Co and the trace siderophile platinum group elements (PGEs) Pt, Ir, and Rh. HH-XRF analyses for Fe, Ni, and Co are summarized in Table 4b, and a compilation of µ-XRF maps showing the distribution of selected elements, is given in Figures 14-18. Analytical results of pLA-ICP-MS are summarized in Table 5.

Kris no. 23606

Measured concentration ranges for kris no. 23606 (Figure 10) are 0.7-4.9 wt% Ni (HH-XRF), <1.4-3.3 wt% Ni (µ-XRF) and ~0.2-0.3 wt% Co (HH-XRF), while no Co at all was detected by µ-XRF. The HH-XRF values for the Co concentrations could lead to infer a slight positive correlation with the

corresponding Ni concentrations. However, as these measurement results are close to the estimated limit of quantification (0.2 wt% for Co) the results bear a high uncertainty and shall not be considered for such interpretation. Micro-XRF mapping (Figure 14) revealed that the visually well-developed pamor pattern of dagger #23606 is also reflected by the distribution of Ni and, in some places, also of other elements (e.g., P, Cr, Cu). The pLA-ICP-MS analysis yielded (Table 5) concentrations of 1.33 wt% for Ni and <0.07 ppm for Co, which agrees with the corresponding µ-XRF data. The latter reinforces the conclusion that for dagger #23606 the HH-XRF results for Co cannot be considered for any further interpretation.
According to its record in the inventory book of the Weltmuseum Wien, kris #23606 was manufactured in the 16th century. In line with the determined composition, the use of the Prambanan meteorite as pamor material can thus be excluded. Therefore, the most plausible explanation for the origin of kris #23606 is that it was forged with non-meteoritic iron metal as pamor material, which likely was smelted from Ni laterite ore of low Co grade based on the compositional data.

Kris no. 23646

Measured concentration ranges for kris no. 23646 (Figure 11) are <0.3-4.8 wt% Ni (HH-XRF), <1.4-3.3 wt% Ni (µ-XRF) and <0.2-0.6 wt% Co (HH-XRF), <0.4-1.0 wt% Co (µ-XRF). Micro-XRF maps (Figure 15) show that Ni is distributed on the blade's surface only along two pamor lines and in one patchy area in the central part of the dagger. This observation is in accordance with the visual description of the blade as being apparently strongly corroded and/or in places covered with a "patina". The µ-XRF maps also reveal the presence of significant amounts of Cr and Cu within the pamor lines and the patchy area, while the distribution of Cu does not overlap with Ni. Thus, during the forging of dagger 23646, Cu-bearing material may have been added on purpose as separate pamor component.
The pLA-ICP-MS analysis yielded for Ni and Co (Table 5) concentrations of 0.35 wt% Ni and <0.07 ppm Co and for the PGE metals Ir and Pt concentrations < DL. In case that all the Ni measured by pLA-ICP-MS is of meteoritic origin, the corresponding Co concentration should be significantly higher than the detection limit of 0.07 ppm. The same line of argumentation holds for the PGEs. Considering the respective detection limits for Ir and Pt of 0.003 ppm and 0.19 ppm and the measured concentrations of 3.42 ppm Ir and 16.7 ppm Pt in the Prambanan sample no. D1483, both elements should be detectable by pLA-ICP-MS if the measured Ni is indeed of meteoritic origin. However, as mentioned above, the surface of the blade of dagger #23646 exhibits in places corrosion features and is covered by a patina, which made it very difficult to position the laser spots correctly at the pre-selected points for analysis. Therefore, it cannot be excluded that spots outside the pamor layers were sampled.
The Ni and Co concentrations measured by HH-XRF and µ-XRF do not exclude a possible meteoritic origin of the pamor material of the dagger, although in the Co vs. Ni diagram, the ore grade values of Ni and Co in nickel laterite deposits (Figure 11) also plot at relatively low Ni concentrations near the bulk Ni/Co ratio line of the Prambanan meteorite. However, because of the absence of detectable amounts of the PGEs Ir and Pt, it is unlikely that the measured Ni is of meteoritic origin.

The age of dagger no. 23646 is unknown, but according to its record in the inventory book of the Weltmuseum Wien, it was acquired in 1886 and thus can be classified as a premodern kris. Considering the laser ablation sampling depth of about 150 µm, it seems very unlikely that Co and the PGEs were completely fractionated from Ni, further supporting the hypothesis that the measured Ni is of terrestrial origin. Therefore, we conclude that dagger #23646 was very likely manufactured with an admixture of Ni-bearing iron that was smelted from nickel laterite ore.

Kris no. 73397

This is one of five kris daggers that were forged in 1904 by a master blacksmith in Yogyakarta, Java. The forging was commissioned by Franz Heger (director of the Ethnographic collection at the former k. k. Hofmuseum in Vienna) with the order to use meteoritic metal (from the local iron meteorite Prambanan) as pamor material (Groneman, 1910). Interestingly, Isaak Groneman himself was present at the blacksmith's working place, where he observed and documented the forging of the daggers (Groneman, 1910).
However, µ-XRF mapping (Figure 16) revealed that dagger no. 73397 does not contain any detectable concentrations of Ni and Co. This observation is confirmed by the just recently reported results of an HH-XRF study of several kris daggers, including kris no. 73397 (Scheiblechner et al., 2024). Although photographic images (Figures 2c, 2h) show a visible pamor pattern, no corresponding distribution of any element could be detected.
Thus, it is evident that, despite the order to use meteoritic metal, the blacksmith forged a dagger with a "fake" meteoritic admixture by using two different malleable iron and/or steel sorts to obtain the pamor pattern on the blade of dagger no. 73397.

Kris no. 119014

Both, HH-XRF and µ-XRF analyses on kris no. 119014 exhibit high concentrations of Ni and Co with measured ranges (Figure 12) of 0.3-16.3 wt% Ni (HH-XRF), <1.4-26.6 wt% Ni (µ-XRF) and <0.2-2.0 wt% Co (HH-XRF), <0.4-6.3 wt% Co (µ-XRF). As an overall feature, the concentrations of Ni and Co are roughly positively correlated, whereas the µ-XRF analyses extend to significantly higher Ni and Co concentrations than the HH-XRF data. This marked difference in the concentration ranges of Ni and Co between HH-XRF and µ-XRF analyses is due to the different spot sizes used by the respective XRF methods. The latter interpretation is supported by the results of the µ-XRF mapping (Figure 17), which reveals that Ni is distributed on the blade's surface within more than 2 mm broad pamor stripes without any detailed internal texture. This observation is also in accordance with the visual description of the blade as being partly corroded and having no well-developed pamor pattern. The µ-XRF maps also reveal the presence of significant amounts of Cr and Cu within the pamor lines. Quantitative analysis results by µ-XRF line scans (Figure 19) performed across sub-mm thick blank metal layers which appear as white "lines" in the corresponding optical image (Figure 17) confirm the overall positive correlation of Ni and Co concentrations, whereas the highest Ni contents are restricted within the narrow metal layers. The line scans also reveal that the contents of Al and Si are anticorrelated with Ni contents, indicating a possible contamination of the corroded blade and/or the presence of remnants of slag inclusions in the host iron metal of the dagger's pamor.

The pLA-ICP-MS analysis yielded Ni and Co concentrations (Table 5) of 2.55 wt% Ni and 0.38 wt% Co, Rh, Ir and Pt metals concentrations < DL, and an apparently high As content, which very likely originates from the use of an arsenic-containing etchant (Groneman, 1910; Necmer et al., 2013). The contents of Ni and Co are significantly lower when compared with the XRF data. However, as in the case of dagger no. 23646, the presence of a "rusty" patina on the blade of dagger no. 119014 made it difficult to position the laser spots correctly at the pre-selected points for analysis and it is thus likely that not all spots were sampled within the pamor layers.

An experimental study based on the forging of knife blades from fragments of the Gebel Kamil meteorite (Ouzillou and Herd, 2023) has shown that the bulk composition of the meteoritic metal did not change significantly through the forging process, with the majority of siderophile elements remaining within 10 rel% of the concentration obtained for the unprocessed meteorite. Thus, even if the blade material analyzed mainly consists of a non-meteoritic component and considering the detection limits of Ir and Pt being 0.003 ppm and 0.19 ppm, the measured concentrations of 3.42

ppm Ir and 16.7 ppm Pt in the Prambanan sample no. D1483 imply that both elements should be detectable by pLA-ICP-MS if the measured Ni is indeed of meteoritic origin (approximately 1 ppm of Ir should be present if all 2.55 wt% Ni present in the dagger originates from the Prambanan iron meteorite). Therefore, we conclude that dagger #119014 was manufactured without the use of a meteoritic admixture. The age of dagger no. 119014 is unknown, but according to its record in the inventory book of the Weltmuseum Wien, it was acquired in 1925. Because of the strongly corroded appearance of the blade and the presence of slag remnants therein, the dagger is very likely a premodern kris, although it cannot be excluded that it was manufactured in the early 20th century.

Kris no. 900382

Among the five krises investigated, dagger no. 900382 exhibits the most intricate and highly decorative pamor pattern (Figures 1e, 2e, and 2j), which apparently was achieved by intense etching. Handheld-XRF and µ-XRF analyses show high to extremely high concentrations of Ni and Co (Figure 13) with measured ranges of <0.3-3.3 wt% Ni (HH-XRF), <1.4-75.3 wt% Ni (µ-XRF) and <0.2-0.7 wt% Co (HH-XRF), <0.2-5.7 wt% Co (µ-XRF). In the Co versus Ni plot (Figure 13), the µ-XRF data show three distinct compositional clusters, whereas in all 3 clusters, the concentrations of Ni and Co have a roughly positive linear correlation. The clusters have approximate concentration ranges of <0.3 to 5 wt% Ni and <0.2 to 1 wt% Co (cluster depicted in the zoom), 5 to 20 wt% Ni and 2 to 4.5 wt% Co (cluster in left half of Figure 13), 50 to 75 wt% Ni and 4 to 6 wt% Co (right half of Figure 13). Two clusters are separated by a gap in the range between 1 and 2 wt% Co, but follow the same Ni/Co trend, while the third cluster differs completely by having much higher Ni contents and higher Ni/Co ratios. All µ-XRF analyses were obtained by four line-scans (labelled A, B, C, and D) performed at different locations of the blade (see optical images in Figures 18a and 18b). The line scan plots (Figure 20) confirm the overall positive correlation of Ni and Co concentrations, whereas the highest Ni contents were measured along line D (Figure 18b, im_2) across a patchy metal area, which apparently represents a pamor layer oriented parallel to the surface of the kris blade. Line scan plots also reveal that the contents of Al and Si are anticorrelated with Ni contents, indicating a possible contamination of the strongly etched blade and/or the presence of remnants of slag inclusions in the host iron metal of the dagger's pamor. Micro-XRF mapping (Figures 18a, 18b) reveal that the visually well-developed pamor pattern of dagger #900382 is also reflected by the distribution of Ni and, in some places, also by the distribution of Cr and Cu.

The pLA-ICP-MS analysis yielded Ni and Co (Table 5) concentrations of 48.2 wt% Ni and 2.13 wt% Co, with a corresponding Ni/Co ratio of 22.6, and PGE metals concentrations of 0.59 ppm Rh, 1.1 ppm Ir, and 3.75 ppm Pt. Thus, dagger no. 900382 is the only kris investigated in this study that contains PGE elements at detectable amounts. For comparison, the measured concentrations in the Prambanan sample D1483 (Table 5) are 9.12 wt% Ni, 0.62 wt% Co (Ni/Co = 14.7), 2.15 ppm Rh, 3.42 ppm Ir, and 16.7 ppm Pt. Considering that the pLA-ICP-MS analysis of dagger no. 900382 was performed on a bulk mixture that contained sampled material from four different spots, it is apparent that its Ni/Co ratio compares well with the meteoritic value and that there is a rough match between inter-element PGE ratios measured in the dagger and the Prambanan sample.

Concerning the possible origin of dagger no. 900382, one thus must consider (i) the high to very high concentrations of Ni and Co measured by µ-XRF, the comparable Ni/Co ratios obtained by pLA-ICP-MS, the PGE concentrations measured by pLA-ICP-MS that roughly match the corresponding ratios measured for the Prambanan iron meteorite, and (ii) the age and provenance of the kris.

The age of dagger no. 900382 is unknown, but according to its record in the inventory book of the Weltmuseum Wien, it originated from the island Sulawesi and was acquired in 1936. Thus, it could be a premodern kris or a modern one that was manufactured at the latest in the early 20th century. In

any case, it is evident that the dagger was manufactured with the admixture of a pamor material that is highly enriched in Ni and Co. The investigation of analog samples in the present study has shown that during the forging process of a kris dagger, Ni can in places be highly enriched up to several tens of wt% at the interface between a pamor layer and the adjacent host iron (see e.g., Figure 5 and Figure 8), but this enrichment is not accompanied by a corresponding enrichment in Co. In contrast to the latter behavior of Co, µ-XRF analyses of dagger #900382 in the compositional range 5-10 wt% Ni have significantly lower Ni/Co ratios when compared to bulk Prambanan (Figure 13). Considering the overall contents of Ni and Co in Ni laterites (Figure 13) and again the µ-XRF analyses in the compositional range 5-10 wt% Ni, we exclude the possibility that no. 900382 is a premodern kris that was forged with a pamor material of Ni-bearing iron that was smelted from nickel laterite ore, even though it is known that many Ni laterites are enriched in PGE metals with a total PGE content of up to several 100 ppb (e.g., Aigelsperger et al., 2016).
Therefore, we conclude that dagger no. 900382 is likely a premodern kris from Sulawesi that was manufactured with an admixture of iron metal from the Prambanan meteorite. However, the alternative hypothesis that the dagger is a modern kris that was manufactured in the late 19th or early 20th century by using a locally produced or imported industrial Ni-metal, which contained up to several wt% Co cannot be totally rejected.

Conclusions

Relying on our study of analog objects that were obtained by a forging procedure similar to the one applied in the production of “real” krises in Indonesia, and on the comparative investigation of original daggers from the Weltmuseum Wien, the following conclusions can be drawn from the use of meteoritic nickel-iron as pamor material in analog samples (items 1-5) and from the investigated kris samples (items 6-8):

1. Meteoritic nickel-iron is in places redistributed within the pamor layers during the repeated process of fire welding and forging, whereas regions with high contents of Ni (up to several tens of wt%) are restricted to a narrow zone along the contact to the adjacent host iron.
2. As an overall feature, the local enrichment of Ni within the pamor layers is restricted to a few layers in the sub-mm range and thus does not affect bulk analyses in the mm range (as e.g., handheld XRF analysis performed in this study).
3. During the whole forging process, there is no significant diffusion of Ni and Co from the pamor layers into the surrounding host iron.
4. Samples taken at consecutive stages of the forging process exhibit an increasing thinning of individual pamor layers in the sub-mm range that is accompanied by a corresponding decrease of the spacing between the layers.
5. In a Co versus Ni plot, almost all HH-XRF analyses performed on polished analog samples plot below the bulk concentrations of these elements in the respective meteoritic admixture, while most HH-XRF analyses performed on etched samples plot at significantly higher Ni/Co ratios. The latter is attributed to selective etching that locally enriches Ni over Co.
6. The main challenges for identifying the presence of a meteoritic component in a kris dagger are linked to the exclusive use of non-destructive methods on the outer surface of the objects. Due to locally varying surface alterations (contamination, corrosion, etching features) on the blades, these analyses may not be representative of the bulk composition of the metal, making it more difficult to draw conclusions about a possible meteoritic origin.
7. The presence of significant amounts of Ni and Co (in the wt% range) in a premodern kris dagger does not imply that it was manufactured with admixture of meteoritic metal.

8. Among the five krises investigated, only dagger no. 900382 was possibly manufactured with an admixture of nickel-iron from the Prambanan iron meteorite based on the high concentrations of the (highly) siderophile elements and a Ni/Co ratio comparable to that of the meteorite. This identification of an admixed meteoritic component may also be further complicated by the admixture of pamor material from multiple sources.

Acknowledgements

We thank Gerald Giester (University of Vienna) for assistance in the pre-selection of kris daggers by HH-XRF measurements, Jani Kuhn-Saptodewo (Weltmuseum Wien) and Robert Blumauer (Weltmuseum Wien) for access to the collection of kris daggers and associated inventory information, Tina-Maria Seyfried (Weltmuseum Wien) for assistance in the loan of kris daggers, Ernst Pernicka (Curt-Engelhorn-Center, Mannheim) and Moritz Numrich (Curt-Engelhorn-Center, Mannheim) for pLA-ICP-MS measurements and data, Goran Batic (Natural History Museum, Vienna) for sample preparation. NJW thanks the Flemish Research Council (FWO) for financial support during this project through an FWO Junior Postdoc grant (Grant nr. 12ZB220N) and the FWO Scientific Prize Climate Research and the Netherlands Research Council (NWO) though a VENI fellowship (Grant nr. VI.Veni.222.354) and an NWO XS research grant (OCENW.XS23.4.125). PC and SG thank FWO for the acquisition of the XRF instrument and the VUB Strategic Research Program for support of the labs. We acknowledge the constructive comments and suggestions of two anonymous reviewers and thank A. J. Timothy Jull for editorial handling.

References

Aiglsperger, T., Proenza J. A., Lewis J. F., Labrador M., Svojtka M., Roja-Puron A., Longo F. and Durisova J. 2016. Critical metals (REE, Sc, PGE) in Ni laterites from Cuba and the Dominican Republic. *Ore Geology Reviews* 73: 127-147.

Baumhauer H. E. 1866. Sur le fer météorique de Prambanan dans le district de Soerakarta (ile de Java). *Archives Néerlandaises des sciences exactes et naturelles* I: 465-468.

Brandstätter F., Migliori A., Visser S., Giester G., Topa D., Kuhnt-Saptodewo S., and Koeberl C. 2016. Meteoritic Iron in Javanese Kris Daggers: A Comparative XRF Study Performed on Original Daggers and Newly Forged Test Objects. 79th Annual Meeting of the Meteoritical Society, abstract #6168.

Bronson B. 1987. Terrestrial and meteoritic nickel in the Indonesian kris. *Journal of the Historical Metallurgy Society* 21(1): 8-15.

Broschat K., Stroebele F., Koeberl C., Eckmann C., and Mertah E. 2022. Iron from Tutankhamun's Tomb. American University in Cairo Press, 76 pp., ISBN: 978-1-61797-997-2.

Buchwald V. F. 1975. Handbook of iron meteorites. Berkeley, California: University of California Press.

Buchwald V.F. 2005. *Iron and steel in ancient times*. Kongelige Danske Videnskabernes Selskab v. 29, p. 1–372.

Butt C.R.M., and Cluzel D. 2013. Nickel Laterite Ore deposits: Weathered Serpentinites. *Elements* 9: 123-128.

Campbell A. J. and Humayun, M. 2005. Compositions of group IVB iron meteorites and their parent melt. *Geochimica et Cosmochimica Acta* 69: 4733-4744.

Cohen E. 1905. *Meteoritenkunde*. Stuttgart, Germany: Schweizerbart.

Comelli D., D'Orazio M., Folco L., El-Halwagy M., Frizzi T., Alberti R., Capogrosso V., Elnaggar, A., Hassan H., Nevin A., Porcelli F., Rashed M. G., and Valentini G. 2016. The meteoritic origin of Tutankhamun's iron dagger blade. *Meteoritics & Planetary Science* 51: 1301-1309.

de Winter N.J., and Claeys P. 2016. Micro X-ray fluorescence (µXRF) line scanning on Cretaceous rudist bivalves: A new method for reproducible trace element profiles in bivalve calcite. *Sedimentology* 64, 231–251. https://doi.org/10.1111/sed.12299

de Winter N., Sinnesael M., Makarona C., Vansteenberge S., and Claeys P. 2017. Trace element analyses of carbonates using portable and micro-X-ray fluorescence: Performance and optimization of measurement parameters and strategies. *Journal of Analytical Atomic Spectrometry* 32: 1211-1223. https://doi.org/10.1039/c6ja00361c

Elias M. 2002. Nickel laterite deposits-geological overview, resources and exploration. In *Giant ore deposits-characteristics, genesis and exploration*, edited by D. Cooke and J. Pongratz, 205-220. Hobart: CODES Special publication 4, University of Tasmania.

Farrokphay S., Cathelineau M., Blancher S.B., Laugier O., and Filippov L. 2019. Characterization of Weda Bay nickel laterite ore from Indonesia. *Journal of Geochemical Exploration* 196: 270-281.

Gemelli M., D'Orazio M., and Folco L. 2014. Chemical analysis of iron meteorites using a hand-held X-ray fluorescence spectrometer. *Geostandards and Geoanalytical Research* 39: 55-69.

Glaus R., Koch J., and Günther D. 2012. Portable Laser ablation sampling device for elemental fingerprinting of objects outside the laboratory with laser ablation inductively coupled plasma mass spectrometry. *Analytical Chemistry* 84: 5358-5364.

Groneman I. 1910. Der Kris der Javaner. *Internationales Archiv für Ethnographie* XIX: 91-161.

Jambon A. 2017. Bronze Age iron: Meteoritic or not? A chemical strategy. *Journal of Archeological Science* 88: 47-53.

Kracher A., Willis J., and Wasson J. T. 1980. Chemical classification of iron meteorites –IX. A new group (IIF), revision of IAB and IIICD, and data on 57 additional irons. *Geochimica et Cosmochimica Acta* 44: 773-787.

McCoy T., Marquardt, A. E., Wasson J. T., Ash R. D., and Vicenzi E. P. 2017. The Anoka, Minnesota iron meteorite as parent to Hopewell meteoritic metal beads from Havana, Illinois. *Journal of Archeological Science* 81: 13-22.

Nečemer M., Lazar T., Šmit Ž., Kump P., and Žužek B. 2013. Study of the provenance and technology of Asian kris daggers by application of X-ray analytical techniques and hardness testing. *Acta Chimica Slovenica* 60: 351-357.

O'Connor, S.J. 1975. Iron Working as Spiritual Inquiry in the Indonesian Archipelago. *History of Religions 14*, 173-190.

Ouzillou M. M. and Herd C. D. K. 2024. Does the composition of meteoritic metal change with forging? An experimental study. *Meteoritics & Planetary Science* 59: 1495-1505.

Numrich M., Schwall C., Lockhoff N., Nikolentzos K., Konstantinidi-Syvridi E., Cultraro M., Horejs B., and Pernicka E. 2023. Portable laser ablation sheds light on Early Bronze Age gold treasures in the old world: New insights from Troy, Poliochni, and related finds. *Journal of Archeological Science* 149: 105694.

Rousseau, R.M. 2001. Detection limit and estimate of uncertainty of analytical XRF results. *Rigaku Journal* 18: 33–47.

Salvemini F., Grazzi F., Kardjilov N., Manke I., Scherillo A., Roselli M.G. and Zoppi M. 2020. Non-invasive characterization of ancient Indonesian Kris through neutron methods. *The European Physical Journal Plus*, *135*, pp.1-25, https://doi.org/10.1140/epjp/s13360-020-00452-2.

Rasmussen K. L., Malvin D. J., and Wasson J. T. 1988. Trace Element Partitioning between Taenite and Kamacite; Relationship to the Cooling Rates of Iron Meteorites. *Meteoritics* 23: 107-112.

Scheiblechner W., Schubert W. D., Strobl S., and Haubner R. 2022. A heavenly sword – forging a Campo del Cielo meteorite. *Practical Metallography* 59: 445-458.

Scheiblechner W., Strobl S., and Haubner R. 2024. Analysen an alten Kris-Dolchen sowie Nachschmiedung eines Dolchs. *BHM Berg- und Hüttenmännische Monatshefte* 169: 510-515.

Strobl S., Scheiblechner W., and Haubner R. 2023. Metallographic preparation of a composite of meteorite iron, steel, pure iron, and nickel manufactured by the Damascus technique. *Practical Metallography* 60: 556-568.

UNESCO Intangible Cultural Heritage 2008. Indonesian Kris. https://ich.unesco.org/en/RL/indonesian-kris-00112 (accessed 04-08-2024).

Van der Ent A. Baker, A. J. M., Van Balgooy M. M. J., and Tjoa A. 2013. Ultramafic nickel laterites in Indonesia (Sulawesi, Halmahera): Mining, nickel hyperaccumulators and opportunities for phytomining. *Journal of Geochemical Exploration* 128: 72-79.

Visser S. 2021. Iron of the Gods. Self-published by S. Visser, ISBN 978-94-643370-3-7.

Wasson J. T. 1985. Meteorites: Their Record of Early Solar System History. New York, W. H. Freeman and Company, 267 pp., ISBN 0-7167-1700-X.

Wasson J. T., Choi B. G., Jerde E. A., and Ulff-Møller F. 1998. Chemical classification of iron meteorites: XII. New Members of the Magmatic Groups. *Geochimica et Cosmochimica Acta* 62: 715-724.

Wasson J. T., Huber H., and Malvin D. J. 2007. Formation of IIAB iron meteorites. *Geochimica et Cosmochimica Acta* 71: 760-781.

Wasson J. T. 2017. Formation of non-magmatic iron-meteorite group IIE. *Geochimica et Cosmochimica Acta* 197: 396-416.

Zhang Y., Qie J., Wang X. F., Cui K., Fu T., Wang J., and Qi, Y. 2020. Mineralogical Characteristics of the Nickel Laterite, Southeast Ophiolite Belt, Sulawesi Island, Indonesia. *Mining, Metallurgy & Exploration* 37: 79-91.

Figure captions:

Figure 1: Photographs of Indonesian kris daggers from the Weltmuseum Wien with inventory numbers 23606 (a), 23646 (b), 73397 (c), 119014 (d) and 900382(e).

Figure 2: Selected photographic close-ups located at the handle to blade transition of kris daggers with inventory numbers 23606 (a), 23646 (b), 73397 (c), 119014 (d) and 900382 (e).

Figure 2 (continued): Selected photographic close-ups of kris blades located at the central part of daggers with inventory numbers 23606 (f), 23646 (g), 73397 (h), 119014 (i) and 900382 (j).

Figure 3: Schematic view of the making of a kris analog sample from puddle iron and meteoritic metal. (a) meteorite sample enveloped by puddle iron, (b) fire welding, (c) forging into a bar, (d) folding, (e) fire welding, (f) forging between two layers of puddle iron, (g) final product (roughly grinded and etched with $FeCl_3$).

Figure 4: High contrast backscattered electron images (BE) and X-ray maps showing the distribution of Ni in selected areas from analog samples I (a), II (b), and III (c).

Figure 5: Backscattered electron image of analog sample I (see also Figure 4) showing two meteoritic layers in a matrix of inclusion-rich puddle iron. Selected EMP-analyses performed at the contact zone between puddle iron and meteoritic layers (nos. 3-6, 14-17) and within the latter one (nos. 8-10) reveal that Ni and Co were locally redistributed during the repeated process of fire welding and forging.

Figure 6: Co versus Ni plot for HH-XRF measurements (diamond symbols) and EMP analyses (black dots) performed on polished analog test samples that were forged from puddle iron with an admixture of the meteorites Campo del Cielo (I) Gibeon (II, III). Filled diamond symbols correspond to HH-XRF measurements performed on unpolished etched samples. Dashed lines show the bulk Ni/Co ratio of Campo del Cielo (Kracher et al. 1980) and Gibeon (Wasson and Kallemeyn 2002).

Figure 7: Backscattered electron images of subsamples that were taken at different stages during the forging process of the analog kris dagger (sample IV) that was manufactured from steel CK52 and a pamor material. The latter was forged as a composite consisting of meteoritic iron (90 vol% Campo

del Cielo, 10 vol% Gibeon and steel ST37. (a) Cross-section of the pamor material (sample IV-0) that consists in total of 9 meteoritic layers (met) alternating with layers of steel ST37. (b) One pamor layer of sample IV-1 hosted by steel CK52 and consisting of alternating layers of meteoritic iron and steel ST37. (c) Sample IV-2 exhibiting 2 thin pamor layers (pam) set in steel CK52. (d) Sample IV-3 exhibiting 4 thin pamor layers (pam) set in steel CK52. Note that image (c) and (d) have the same scale.

Figure 8: Co versus Ni plot for EMP analyses performed on several subsamples of analog kris dagger (sample IV) that was manufactured from steel with a meteoritic admixture (90 vol% Campo del Cielo, 10 vol% Gibeon). The subsamples comprise the primary pamor material IV-0 and samples IV-1 to IV-3 that were taken at different stages of the forging process. Subsamples IV-5 and IV-6 are from the dagger's tang and tip, respectively. Dashed lines show the bulk Ni/Co ratio of the iron meteorites Campo del Cielo (Kracher et al. 1980) and Gibeon (Wasson and Kallemeyn 2002).

Figure 9: Backscattered electron image of sample IV-6 that was taken from the tip of analog dagger IV. The image shows two meteoritic pamor layers (pam) in a matrix of steel CK52 exhibiting a granular texture, whereas the different shades of gray are due to orientation effects and do not reflect different chemical compositions. Selected EMP-analyses reveal that the concentrations of Ni and Co in the pamor layers of the dagger's tip are significantly lower than the corresponding bulk values for these elements in meteorites Campo del Cielo and Gibeon that were used to make the pamor material of dagger IV (see also Figure 8).

Figure 10: Co versus Ni plot for µ-XRF (squares) and HH-XRF (triangles) measurements performed on the blade of kris dagger no. 23606. Error bars represent 2-sigma standard deviations calculated from analyzed standards as pooled deviation and from the counting statistics of single analyses for µ-XRF and HH-XRF measurements, respectively. Open circles indicate the range of ore grade values of Ni and Co in nickel laterite deposits (Elias, 2002). The dashed line shows the bulk Ni/Co ratio of the Prambanan meteorite (Kracher et al., 1980).

Figure 11: Co versus Ni plot for µ-XRF (squares) and HH-XRF (triangles) measurements performed on the blade of kris dagger no. 23646. Error bars represent 2-sigma standard deviations calculated from analyzed standards as pooled deviation and from the counting statistics of single analyses for µ-XRF and HH-XRF measurements, respectively. Open circles indicate the range of ore grade values of Ni and Co in nickel laterite deposits (Elias 2002). The dashed line shows the bulk Ni/Co ratio of the Prambanan meteorite (Kracher et al., 1980).

Figure 12: Co versus Ni plot for µ-XRF (squares) and HH-XRF (triangles) measurements performed on the blade of kris dagger no. 119014. Error bars represent 2-sigma standard deviations calculated from analyzed standards as pooled deviation and from the counting statistics of single analyses for µ-XRF and HH-XRF measurements, respectively. Open circles indicate the range of ore grade values of Ni and Co in nickel laterite deposits (Elias, 2002). Dashed lines show the bulk Ni/Co ratio of the Prambanan meteorite (Kracher et al., 1980).

Figure 13: Co versus Ni plot for µ-XRF (squares) and HH-XRF (triangles) measurements performed on the blade of kris dagger no. 900382. Error bars represent 2-sigma standard deviations calculated from analyzed standards as pooled deviation and from the counting statistics of single analyses for µ-XRF and HH-XRF measurements, respectively. Open circles indicate the range of ore grade values of Ni and Co in nickel laterite deposits (Elias, 2002). Dashed lines show the bulk Ni/Co ratio of the Prambanan meteorite (Kracher et al., 1980).

Figure 14: X-ray maps (produced by µ-XRF scanning) showing the distribution of Fe, Ni, and Cr within a selected area (red rectangle) on the blade of dagger no. 23606, im = optical image. For each element, the maps exhibit only relative concentrations ranging from low (blue color) to high (red

color).

Figure 15: X-ray maps (produced by µ-XRF scanning) showing the distribution of Fe, Ni, Cr and Cu within a selected area (red rectangle) on the blade of dagger no. 23646, im = optical image. For each element, the maps exhibit only relative concentrations ranging from low (blue color) to high (red color).

Figure 16: X-ray maps (produced by µ-XRF scanning) showing the distribution of Fe, Ni, Cr and Mn within a selected area (red rectangle) on the blade of dagger no. 73397, im = optical image. For each element, the maps exhibit only relative concentrations ranging from low (blue color) to high (red color).

Figure 17: X-ray (produced by µ-XRF scanning) maps showing the distribution of Fe, Ni, Cr and Cu within a selected area (red rectangle) on the blade of dagger no. 119014, im = optical image. For each element, the maps exhibit only relative concentrations ranging from low (blue color) to high (red color). Red arrows in the image show the locations of line scans A, B, and C.

Figures 18a and 18b: X-ray maps (produced by µ-XRF scanning) showing the distribution of Fe, Ni, Cr and Cu within three selected areas (red rectangles) on the blade of dagger no. 900382, im = optical mage. For each element, the maps exhibit only relative concentrations ranging from low (blue color) to high (red color). Red arrows in the video images show the locations of line scans A, B, C and D.

Figure 19: Plot of µ-XRF line scans performed along selected lines A, B, and C on the blade of dagger 119014 (see Figure 17). The concentrations of Al, Si, and As were not quantified by a matrix-matched calibration and should be considered as one-standard quantified data. The line scans exhibit an overall positive correlation of Ni and Co and in places significant amounts of Al and Si, which indicates the presence of slag inclusions in the host iron metal of the dagger's pamor lines.

Figure 20: Plot of µ-XRF line scans performed along selected lines A, B, C and D on the blade of dagger 900382 (see Figure 18). The concentrations of Al, Si, and As were not quantified by a matrix-matched calibration and should be considered as one-standard quantified data. The line scans exhibit an overall positive correlation of Ni and Co and in places significant amounts of Al and Si, which indicates the presence of slag inclusions in the host iron metal of the dagger's pamor line.

Table 1. Indonesian kris daggers of the Weltmuseum Wien investigated by X-ray fluorescence (XRF) spectroscopy and portable laser ablation combined with laboratory-based inductively-coupled plasma mass spectrometry (pLA-ICP-MS).

inventory no.	year[1]	former collection[2]	length (in cm)[3]		provenance	approximate age[4]	investigated by		
			L1	L2			HH-XRF[5]	μ-XRF[6]	pLA-ICP-MS
23606	1886	J. A. Dieduksman	31	39.5	Java	manufactured in 1597	yes	yes	yes
23646	1886	J. A. Dieduksman	33.5	43	Java	not given	yes	yes	yes
73397	1905	F. Heger	36	43	Java	manufactured in 1904	no	yes	no
119014	1925	K. Merio	27.5	37.5	Java	not given	yes	yes	yes
900382	1936	unknown	29.5	36.5	Sulawesi	not given	yes	yes	yes

[1]Year of acquisition by the Weltmuseum Wien.

[2]Before acquisition by the Weltmuseum Wien.

[3]L1 = length of blade, L2 = length of blade plus hilt.

[4]Age information from entries in the inventory book of the Weltmuseum.

[5]HH-XRF = handheld XRF.

[6]μ-XRF = Tornado micro-XRF instrument.

Table 2. Materials used for the forging of analogue test objects.

Name/abbreviation	Material	Chemical group	Bulk chemistry			Reference
			Ni	Co	Ni/Co	
Campo del Cielo	Iron meteorite, Og[1]	IAB	6.7	0.5	13.4	Wasson and Kallemeyn (2002)
Gibeon	Iron meteorite, Of[2]	IVA	7.8	0.4	19.5	Kracher and Wasson (1980)
Puddle Iron	Wrought iron with slag inclusions					Electron microprobe analysis (this study)[3]
ST37[4]	Low-carbon steel[4]					www.murraysteelproducts.com
CK52[5]	Low-carbon steel[5]					www.murraysteelproducts.com

[1]Og = coarse octahedrite, kamacite bandwidth 3.0 ± 0.6 mm (Buchwald, 1975).

[2]Of = fine octahedrite, kamacite bandwidth 0.3 ± 0.05 mm (Buchwald, 1975).

[3]Compostional range of metal (six point analyses, wt%): < 0.02 Si, 0.02-0.21 Mn, <0.02-0.08 Cr, <0.02 Co, 0.05-0.11 Ni.

[4]Eqiuvalent to steel S235 having maximum contents (in wt%) of 0.17 C, 1.4 Mn, 0.03 S, 0.55 Cu.

[5]Equivalent to steel ST52-3 having maximum contents (in wt%) of 0.22 C, 0.55 Si, 1.6 Mn, 0.04 S, 0.04 P.

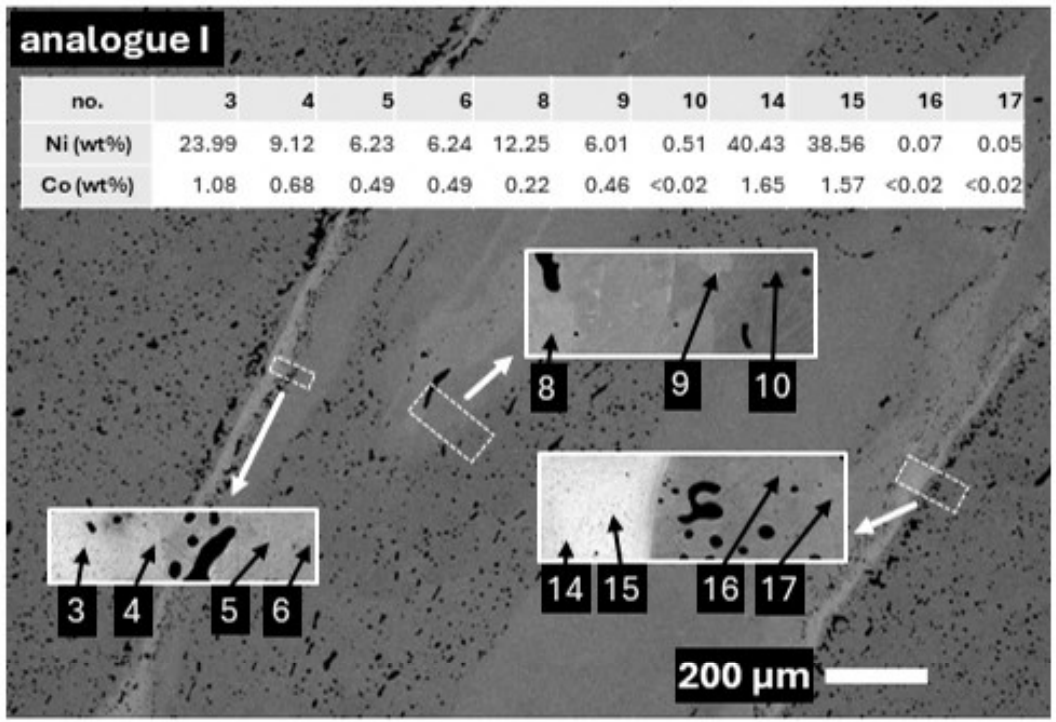

analogue I
no. 3 4 5 6 8 9 10 14 15 16 17
Ni (wt%) 23.99 9.12 6.23 6.24 12.25 6.01 0.51 40.43 38.56 0.07 0.05
Co (wt%) 1.08 0.68 0.49 0.49 0.22 0.46 <0.02 1.65 1.57 <0.02 <0.02
3
4
5
6
8
9
10
14
15
16
17
200 µm

Table 3. Verification of accuracy of calibration (measurements in wt% with the Thermo Scientific Niton Xlt XRF analyzer) for four reference samples.

	carbon steel Fe alloy, Advent Fe 164511		Tool steel NBS 1157		Fe-Ni-Co alloy NBS 1250		Prambanan meteorite NHM no. D1483	
element	´reference[1]	measured	reference[2]	measured	reference[3]	measured	reference[4]	measured
Fe	99.5 ± 0.5	98.9 ± 0.3	80.97 ± 0.06	81.3 ± 0.2	40.5 ± 0.2	41.35 ± 0.08	-	89.4 ± 0.3
Ni	<0.01	<0.3	0.228 ± 0.03	0.172 ± 0.014	37.78 ± 0.1	38.19 ± 0.13	10.1 ± 0.2	9.60 ± 0.06
Co	<0.01	<0.2	0.028 ± 0.002	<0.07	16.1 ± 0.2	14.38 ± 0.06	0.7 ± 0.1	0.82 ± 0.05

[1]www.advent-rm.com

[2]www.nist.gov

[3]www.nist.gov

[4]Kracher et al. (1980)

Table 4a. HH-XRF measurements (element wt%) of analog test materials performed on polished samples I, II, II and etched samples Ic, IIc, IIIc.

sample	n[1]	Fe		Ni		Co	
		min[2]	max[3]	min	max	min	max
I	10	96.7	99.3	<0.3	2.5	<0.2	0.3
Ic	4	86.6	92.4	3.4	8.9	0.3	0.4
II	5	98.3	98.9	0.3	1.0	<0.2	<0.2
IIc	2	83.7	87.0	10.6	13.7	0.2	0.3
III	11	93.0	97.8	1.41	5.8	<0.2	0.4
IIIc	2	71.2	74.5	22.9	26.0	0.4	0.4

[1]Number of spots.

[2]Minum content.

[3]Maximum content.

Table 4b. HH-XRF measurements (element wt%) performed at individual analysis spots located on both sides of the kris blades and on one sample of the Prambanan meteorite (NHM no. D1483).

dagger	n[1]	Fe		Ni		Co	
		min[2]	max[3]	min	max	min	max
23606	9	92.4	96.8	0.7	4.9	<0.2	0.3
23646	6	93.0	98.40	<0.3	4.8	<0.2	0.6
119014	5	79.7	95.3	0.32	16.3	<0.2	2.0
900382	5	88.9	95.9	<0.3	3.3	<0.2	0.6
D1483	2	89.4	89.5	9.5	9.7	0.8	0.8

[1]Number of spots.

[2]Minum content.

[3]Maximum content.

Table 5. Portable laser ablation combined with laboratory-based inductively-coupled plasma mass spectrometry (pLA-ICP-MS) of four kris daggers and one sample of the Prambanan meteorite.

object		dagger				Prambanan	
Element[1]	DL[2]	23606	23646	119014	900382	NHM-D1483	Bulk[3]
Fe	0.0047	98.4	99.3	96.0	49.3	90.2	-
Ni	0.00013	1.33	0.35	2.55	48.2	9.12	10.14
Co	0.000007	<DL	<DL	0.38	2.13	0.62	0.70
Mn	0.5	93.0	864	95.9	15.7	18.0	-
Cu	0.73	508	302	906	2110	547	236
Rh	0.003	<DL	<DL	<DL	0.59	2.15	-
W		19.8	4.12	23.7	1.59	2.11	-
Ir	0.003	<DL	<DL	<DL	1.10	3.42	4.2
Pt	0.019	<DL	<DL	<DL	3.75	16.7	-
Au	13.76	<DL	<DL	<DL	15.3	<DL	-
Zn	2	265	279	<DL	361	<DL	-
As	1.12	1100	1250	11800	1130	6.93	7.5
Mo	1.12	12.4	10.9	118	12.7	16.6	-
Ag	0.13	2.5	17.9	13.3	<DL	<DL	-
Sn	0.27	177	21.7	56.4	12.3	4.97	-
Sb	0.48	27.3	27.8	37.4	113	14.7	-
Te	0.77	<DL	2.52	0.88	<DL	<DL	-
Se		61.7	92.2	113	50.3	150	-
Pb	0.12	35.5	28.7	79.5	16.3	12.0	-
Bi	0.02	1.21	2.25	0.33	<DL	<DL	-
Ni/Co	-	-	-	6.7	22.6	14.7	14.5

[1]Element concentrations of Fe, Ni and Co in wt%, all other elements in ppm.

[2]DL = Limit of detection.

[3]Bulk data from Kracher et al. (1980).


a
10 cm

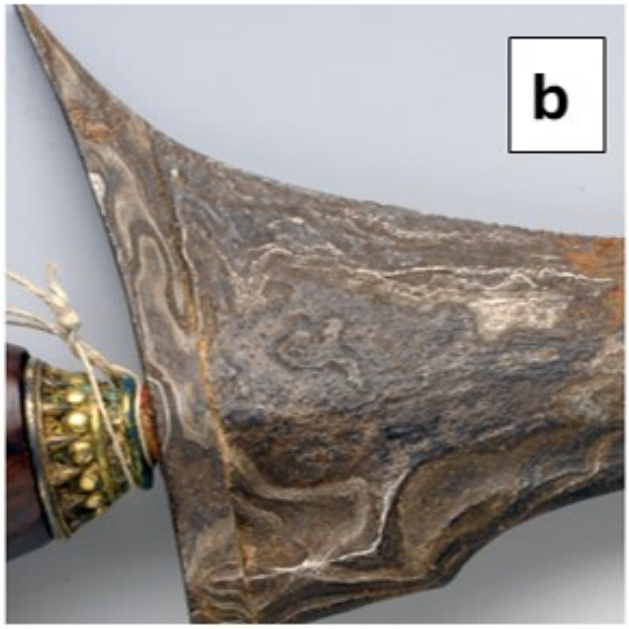

b
10 cm


c
10 cm


d
10 cm


e
10 cm


a


b


c


d


e

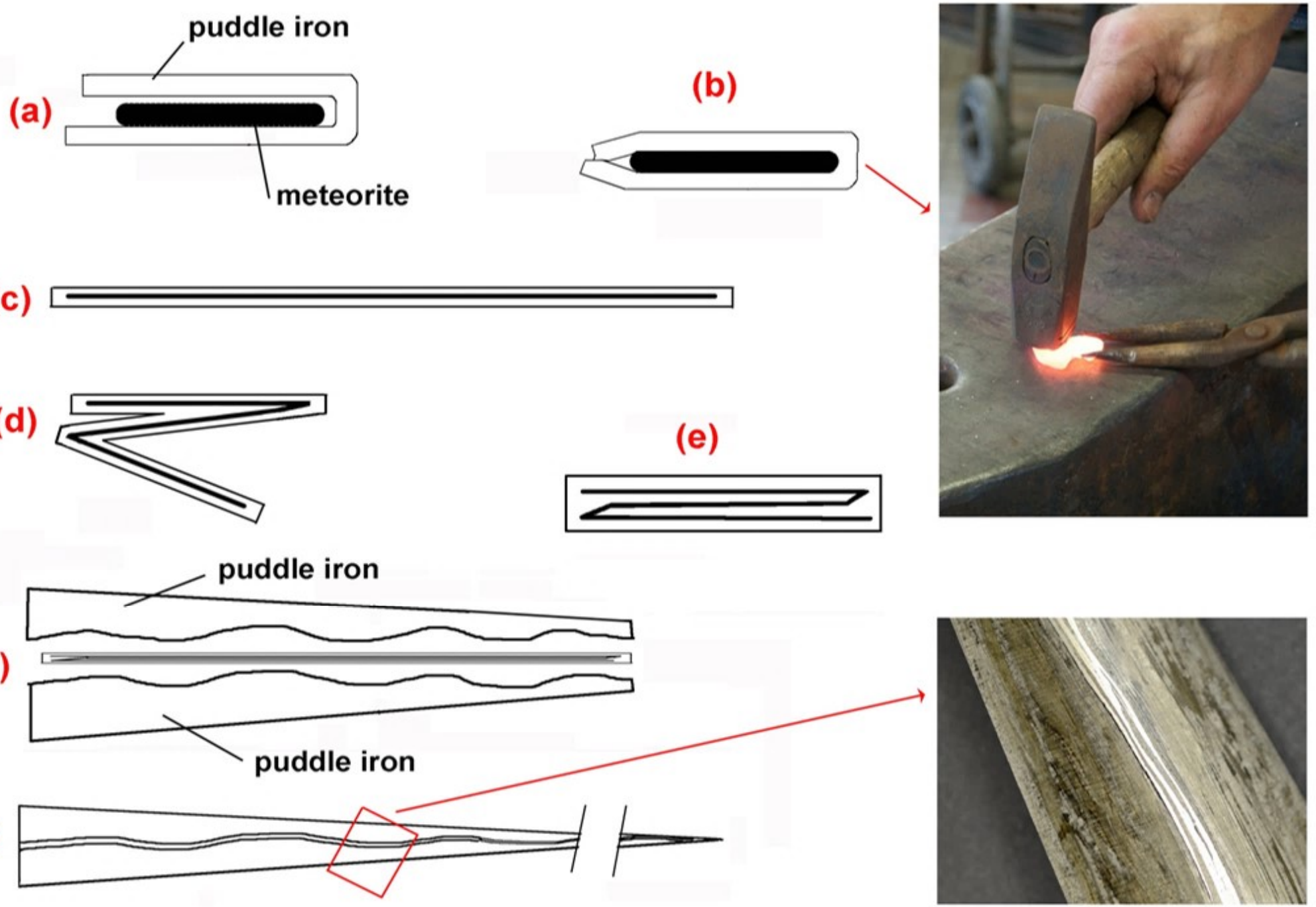

f

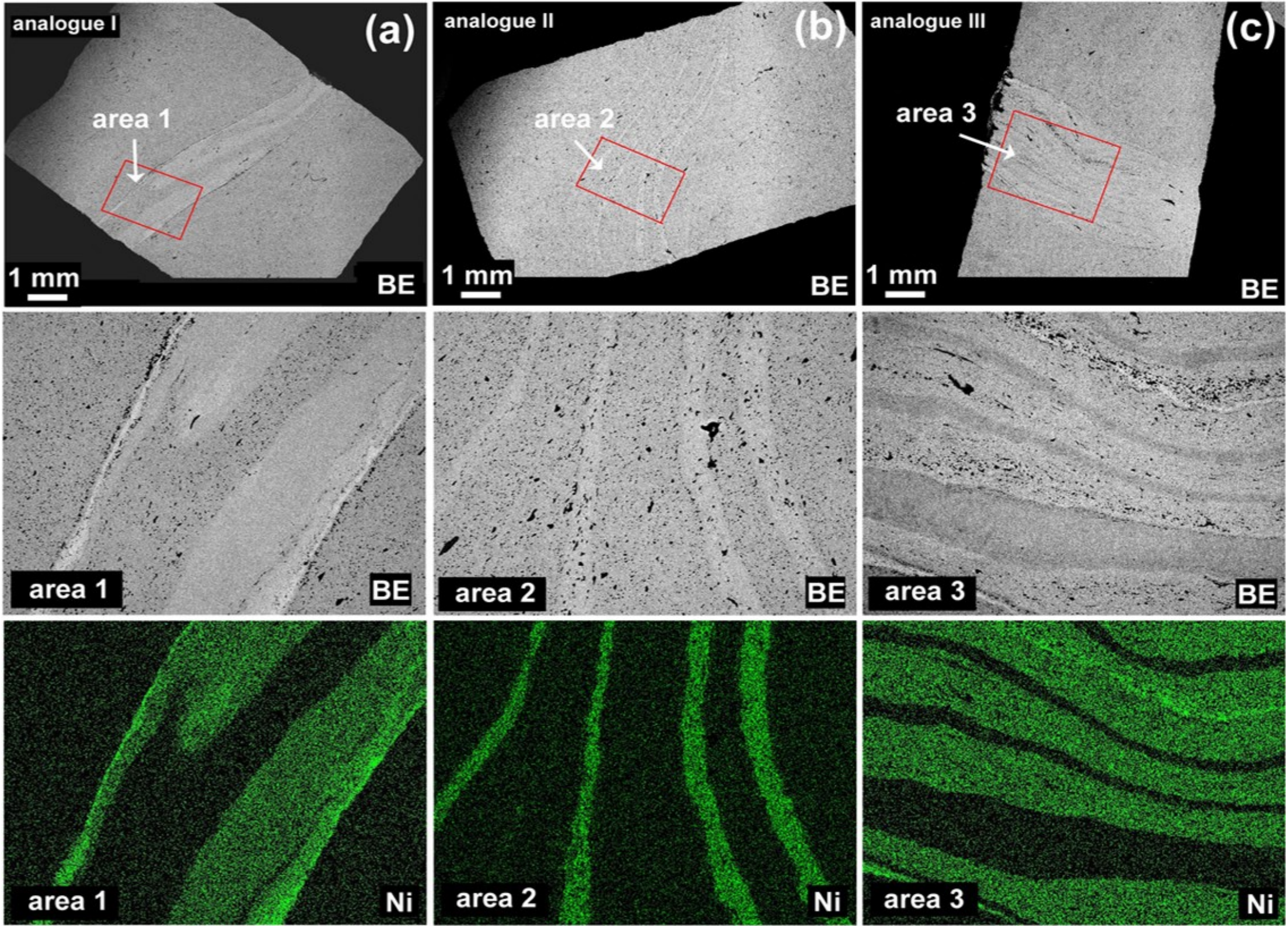

g

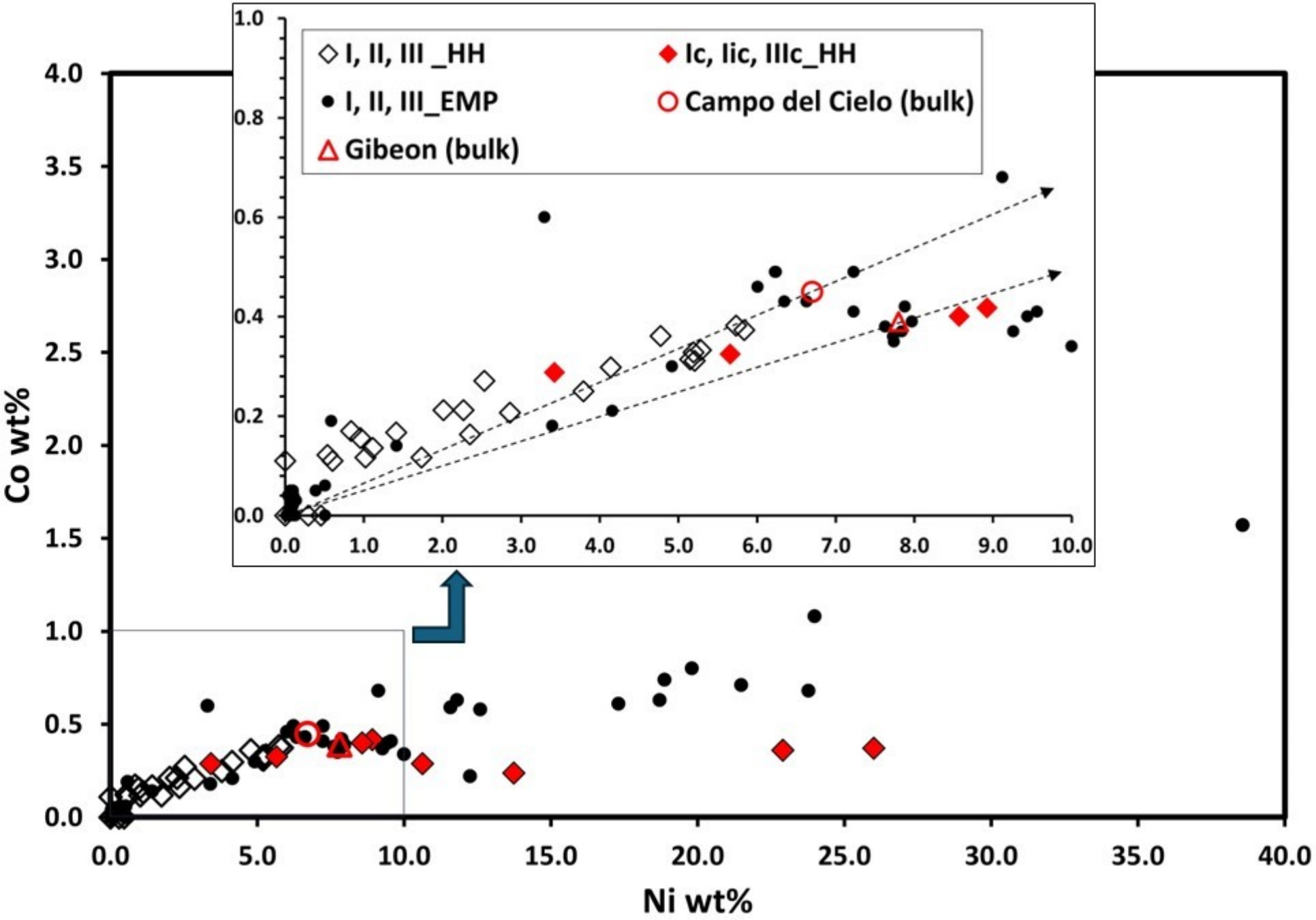

h

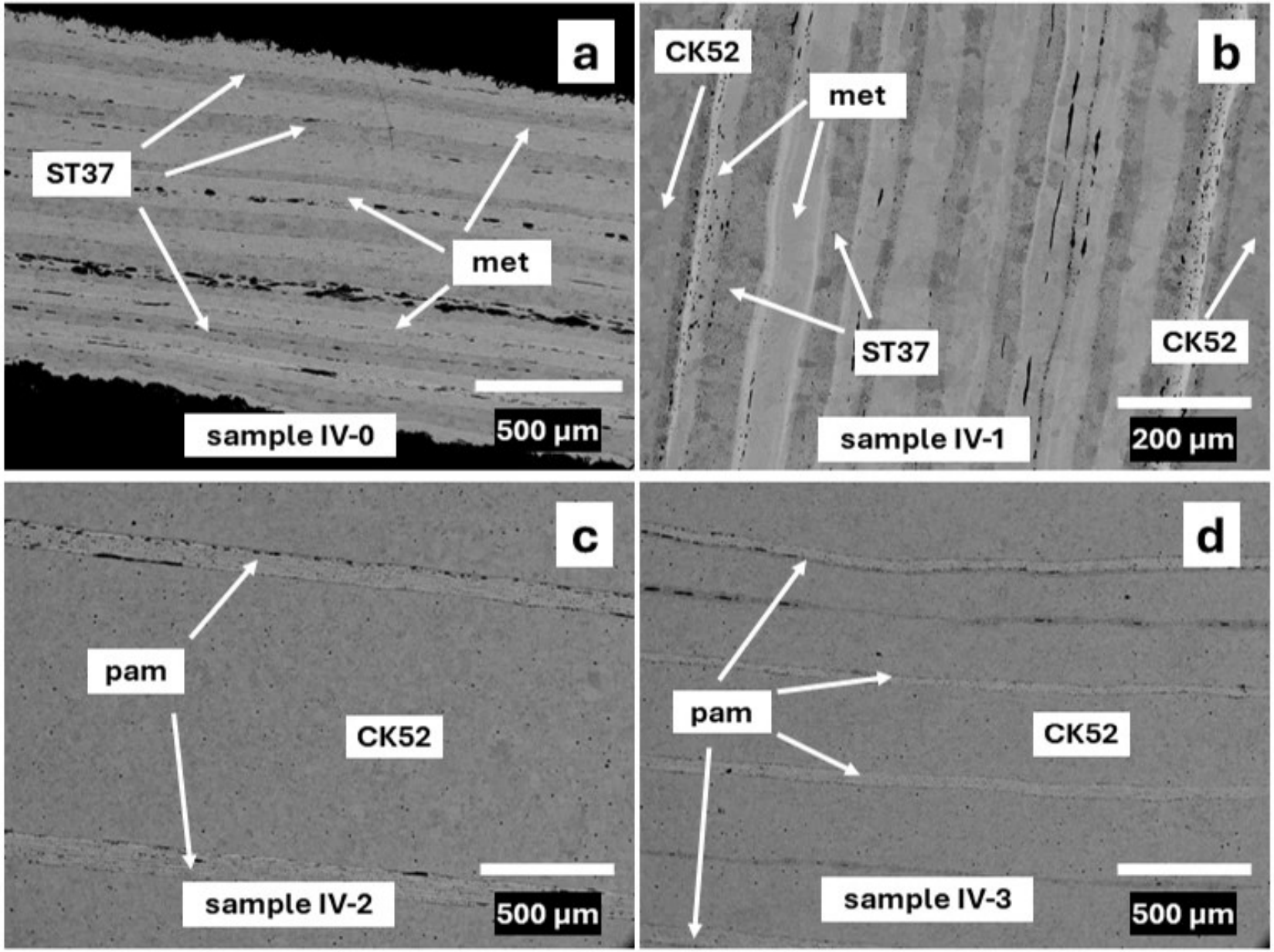

i

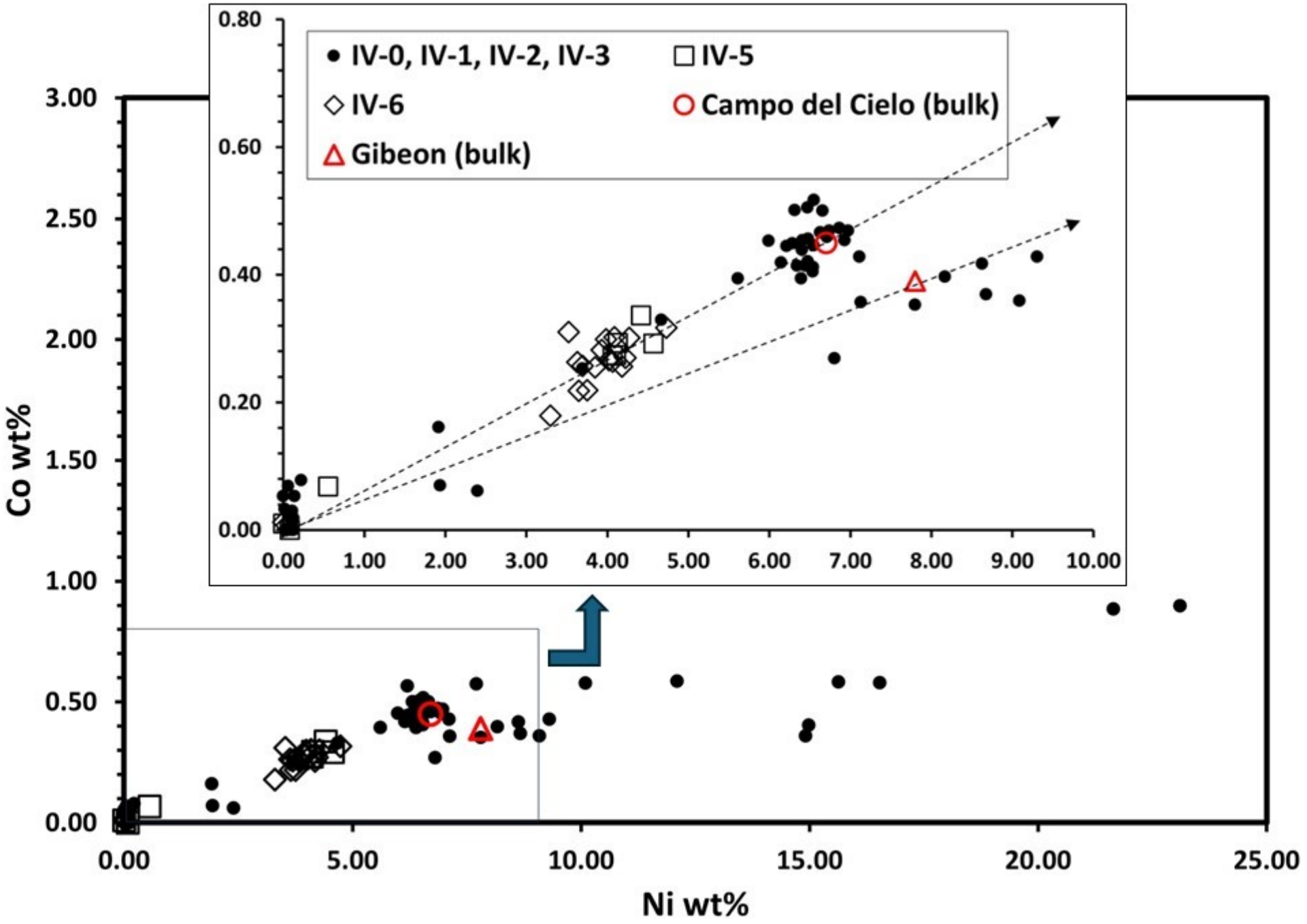

j

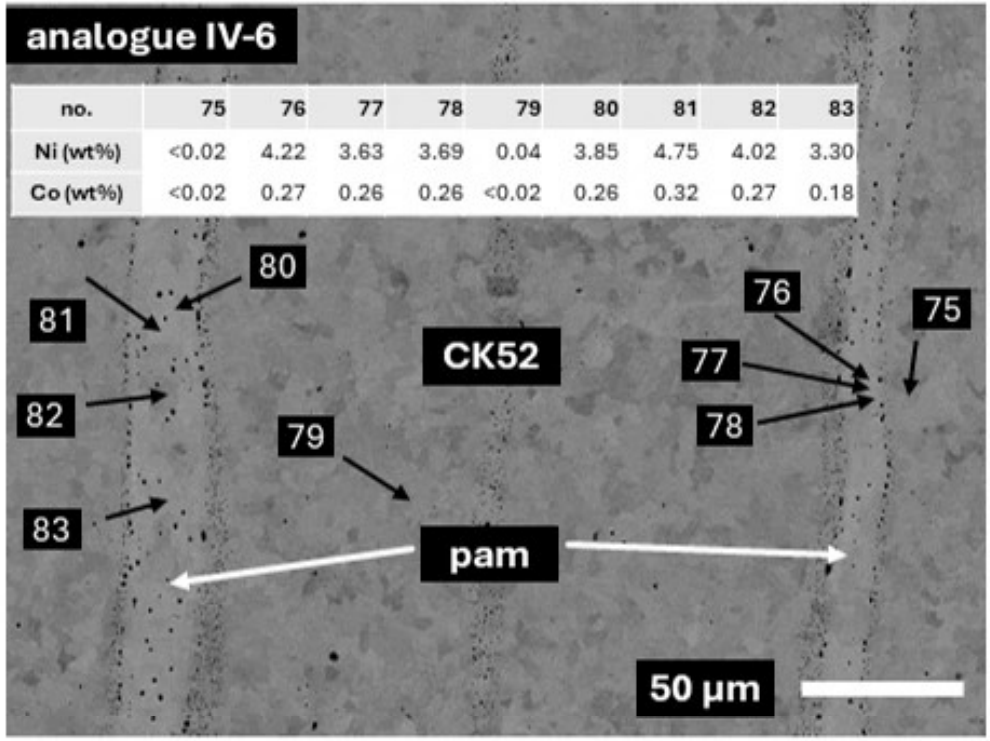

puddle iron
(a)
meteorite
(b)
(c)
(d)
(e)
puddle iron
(f)
puddle iron
(g)

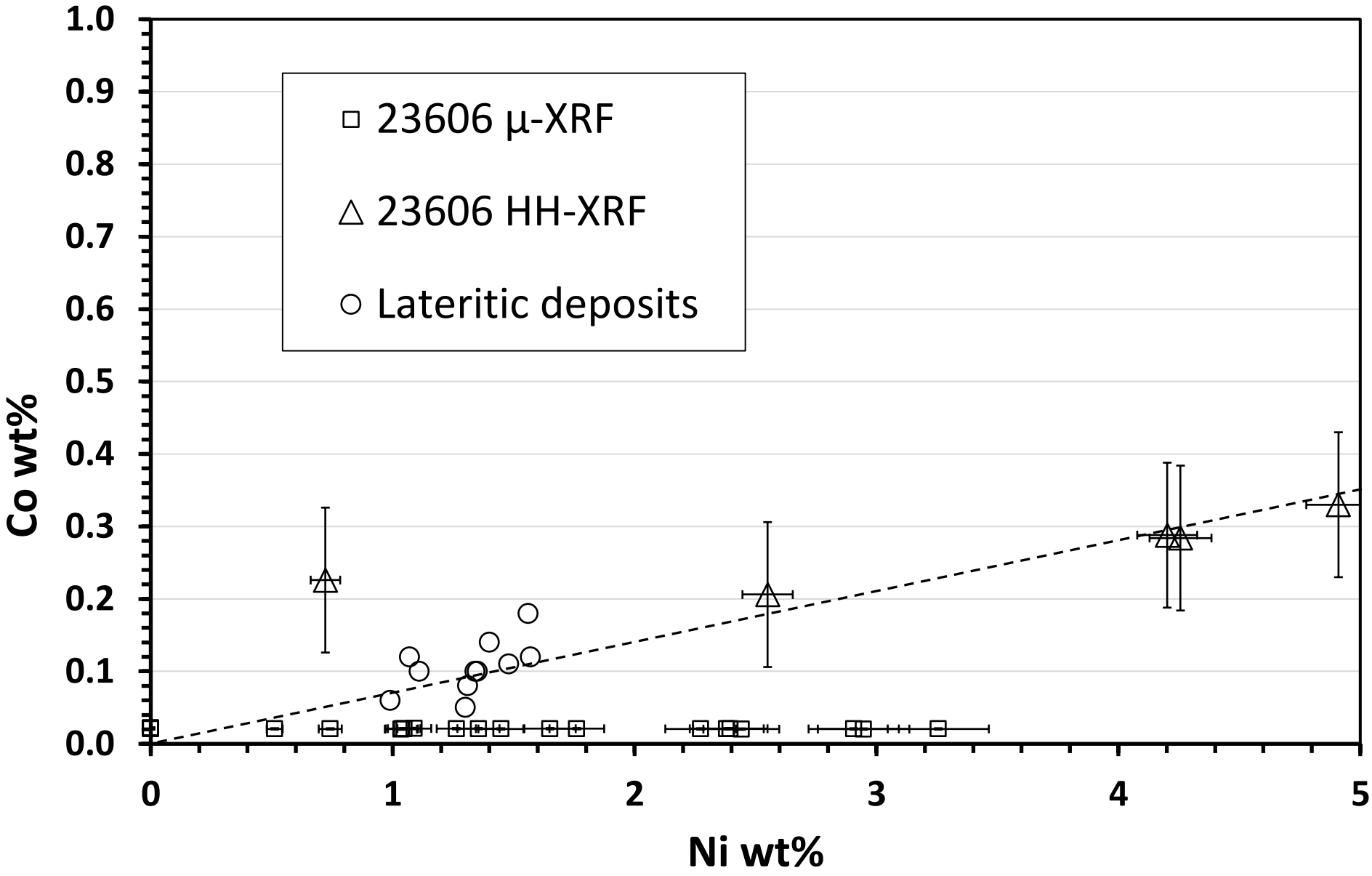

analogue I
(a)
area 1
1 mm
BE
analogue II
(b)
area 2
1 mm
BE
analogue III
(c)
area 3
1 mm
BE
area 1
BE
area 2
BE
area 3
BE
area 1
Ni
area 2
Ni
area 3
Ni

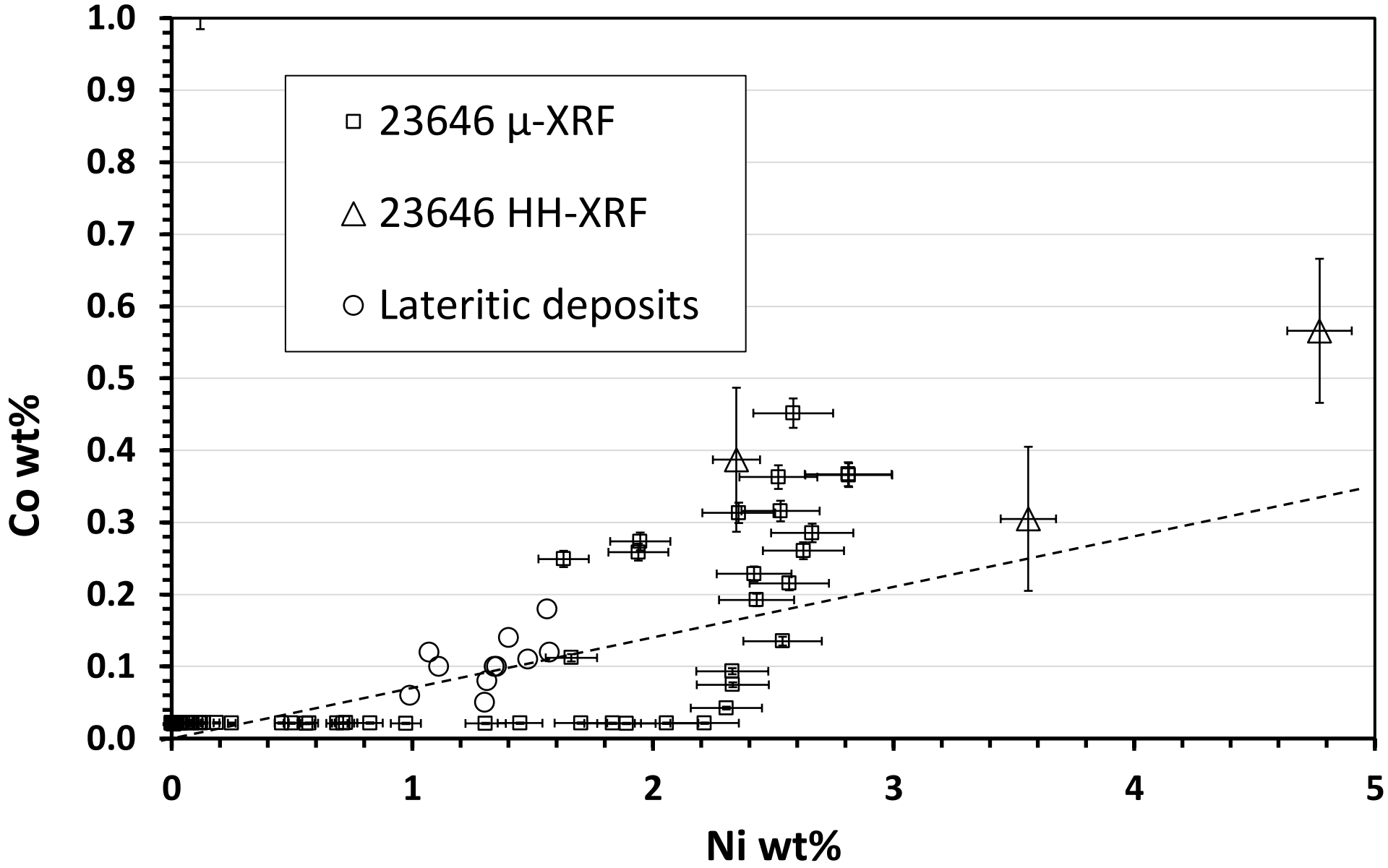

I, II, III _HH
Ic, IIc, IIIc_HH
I, II, III_EMP
Campo del Cielo (bulk)
Gibeon (bulk)
Co wt%
Ni wt%
0.0
0.5
1.0
1.5
2.0
2.5
3.0
3.5
4.0
0.0
5.0
10.0
15.0
20.0
25.0
30.0
35.0
40.0
0.2
0.4
0.6
0.8
1.0
6.0
7.0
8.0
9.0

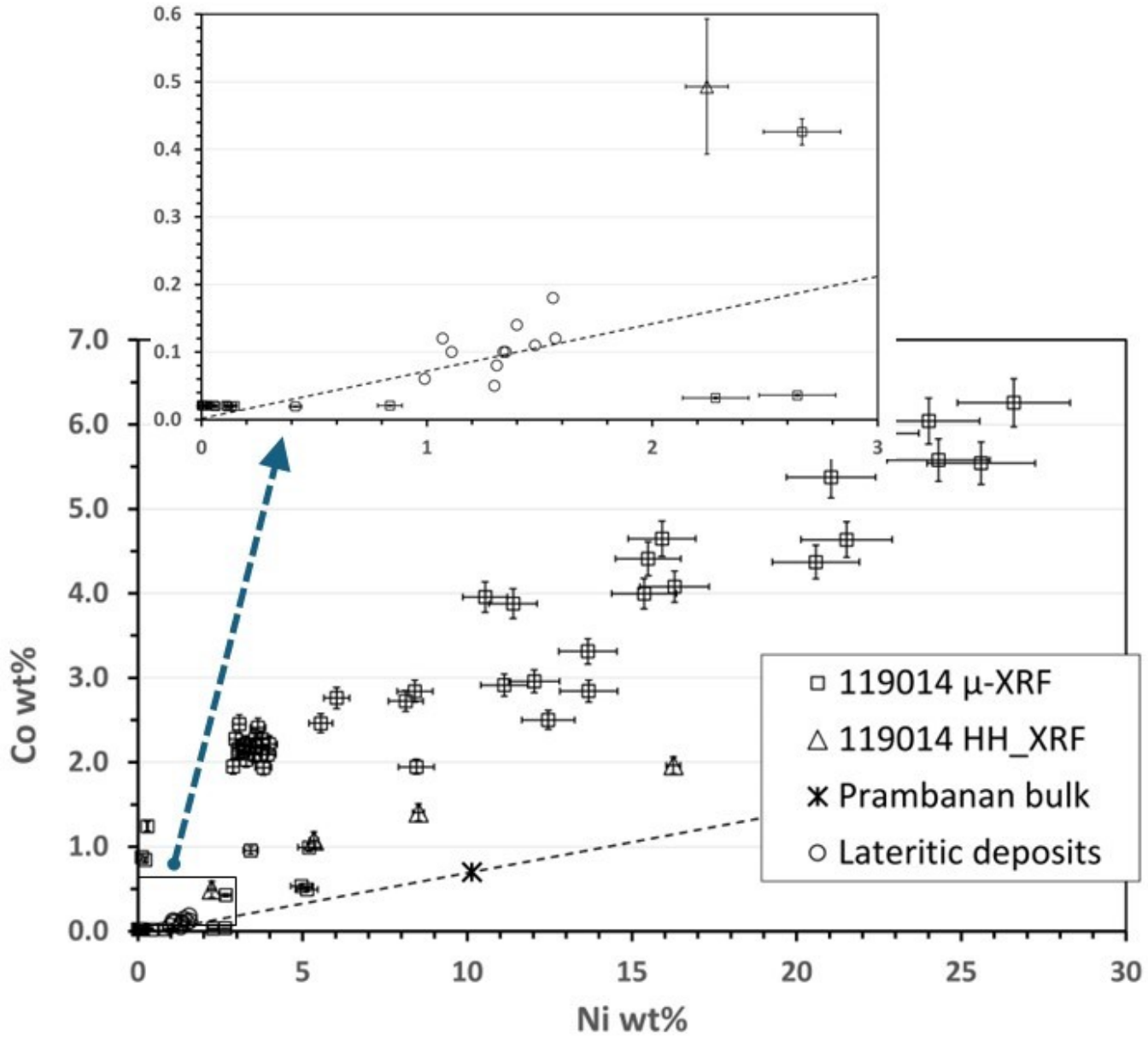

a
ST37
met
sample IV-0
500 µm
b
CK52
met
ST37
CK52
sample IV-1
200 µm
c
pam
CK52
sample IV-2
500 µm
d
pam
CK52
sample IV-3
500 µm

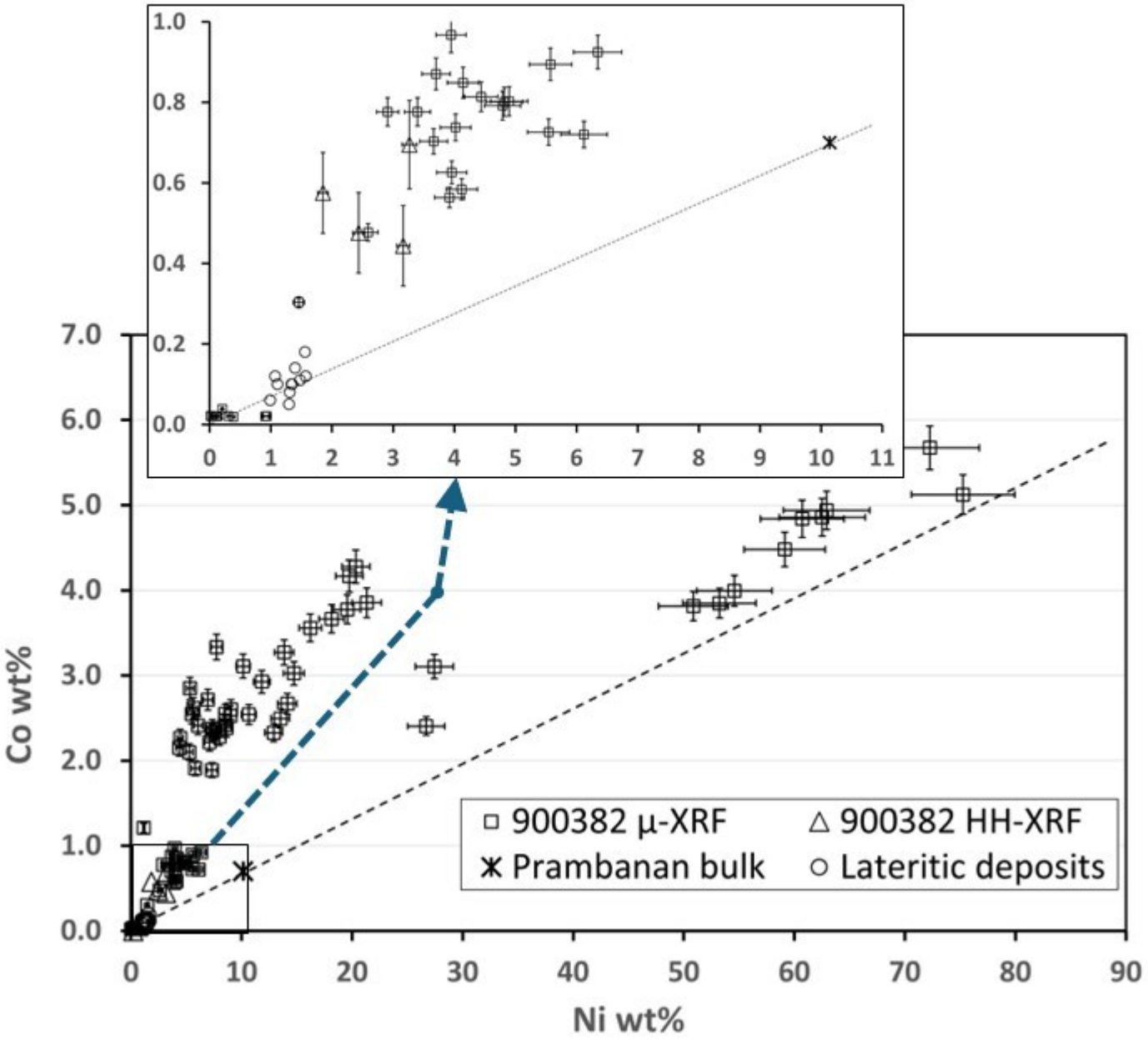

IV-0, IV-1, IV-2, IV-3
IV-5
IV-6
Campo del Cielo (bulk)
Gibeon (bulk)
Co wt%
Ni wt%
0.00
0.50
1.00
1.50
2.00
2.50
3.00
0.00
5.00
10.00
15.00
20.00
25.00
0.00
0.20
0.40
0.60
0.80
0.00
1.00
2.00
3.00
4.00
5.00
6.00
7.00
8.00
9.00
10.00


analogue IV-6
no. 75 76 77 78 79 80 81 82 83
Ni (wt%) <0.02 4.22 3.63 3.69 0.04 3.85 4.75 4.02 3.30
Co (wt%) <0.02 0.27 0.26 0.26 <0.02 0.26 0.32 0.27 0.18
80
81
82
83
79
CK52
76
75
77
78
pam
50 µm


1.0
0.9
0.8
0.7
0.6
0.5
0.4
0.3
0.2
0.1
0.0
Co wt%
0
1
2
3
4
5
Ni wt%
23606 µ-XRF
23606 HH-XRF
Lateritic deposits


23646 µ-XRF
23646 HH-XRF
Lateritic deposits
Co wt%
Ni wt%
0.0
0.1
0.2
0.3
0.4
0.5
0.6
0.7
0.8
0.9
1.0
0
1
2
3
4
5


Co wt%
Ni wt%
0.0
1.0
2.0
3.0
4.0
5.0
6.0
7.0
0
5
10
15
20
25
30
0.0
0.1
0.2
0.3
0.4
0.5
0.6
0
1
2
3
119014 µ-XRF
119014 HH_XRF
Prambanan bulk
Lateritic deposits


Co wt%
Ni wt%
0.0
1.0
2.0
3.0
4.0
5.0
6.0
7.0
0
10
20
30
40
50
60
70
80
90
900382 µ-XRF
900382 HH-XRF
Prambanan bulk
Lateritic deposits
0.0
0.2
0.4
0.6
0.8
1.0
0
1
2
3
4
5
6
7
8
9
10
11